

Optimal Synthesis of Refrigeration Cycles and Selection of Refrigerants

Shankar Vaidyaraman and Costas D. Maranas

Dept. of Chemical Engineering, The Pennsylvania State University, University Park, PA 16802

The optimal synthesis of the refrigeration configuration and the selection of the best refrigerants that satisfy a set of process cooling duties at different temperatures is addressed. This approach simultaneously selects refrigerants and synthesizes refrigeration structures by minimizing a weighted sum of investment and operating costs. A superstructure representation considers the majority of refrigeration cycle features encountered in real complex multistage refrigeration cycles such as economizers, multiple refrigerants, and heat integration. A novel theoretical treatment of modeling representations and algorithmic improvements is introduced. Results, for example, involving multiple refrigerants, cooling loads, and heat sinks are obtained. Complex, nonintuitive topologies typically emerge as the optimal refrigeration configurations that are better than those obtained when refrigeration synthesis is performed after refrigerant selection.

Introduction

The need for efficient utilization and recovery of energy in chemical processes has been firmly established on both economic and environmental grounds. Refrigeration systems in chemical process plants are complex, energy, and capital intensive utility systems which remove heat from low-temperature process streams and reject it to streams at higher temperature or cooling water at the expense of mechanical work. Most research work in refrigeration systems addresses the refrigeration cycle synthesis problem in isolation of the refrigerant selection. In this work we show that significant cost reduction can be realized by encompassing both objectives within the same unified framework.

A simple vapor compression refrigeration cycle consists of a sequence of evaporation, compression, condensation, and expansion steps. In most cases, refrigeration needs to arise simultaneously for multiple loads at different temperature ranges. This necessitates the need for staged refrigeration cycles with multiple compressors and evaporators to meet the process cooling loads. Even for a single refrigeration load, in many cases, a single refrigeration stage cannot span the entire temperature range between the evaporator and the condenser, either because the required compression ratio is too high or the critical pressure is reached in the condenser. This explains why design alternatives typically need to be explored

involving complex multistage refrigeration cycles utilizing multiple refrigerants for different temperature ranges. This complexity of the topology of refrigeration cycles and the diversity in the selection of refrigerant molecules coupled with the high investment and energy intensive nature of refrigeration cycles motivates the need for the development of systematic procedures for the efficient synthesis of refrigeration cycles.

One of the earlier works addressing the problem of synthesizing minimum cost cascade refrigeration systems is that of Barnes and King (1974). They identified and standardized numerous refrigeration topologies, uncovered a number of trade-offs in the synthesis of multi-stage cycles, and derived a dynamic programming method for identifying good refrigeration system configurations. The advantage of this approach is that it can handle detailed equipment cost correlations and thermophysical property models. However, the number of stages and their operating temperature ranges were determined based on a heuristic procedure and no solution performance guarantees were possible. Later, Cheng and Mah (1980) proposed an interactive procedure for synthesizing refrigeration systems incorporating all the refrigeration features identified by Barnes and King (1974). The refrigerants participating in a cycle were selected based on their allowable operating temperature range and the temperature of the process streams to be cooled. A heuristic based on the aver-

Correspondence concerning this article should be addressed to C. D. Maranas.

age compression work and the amount of vapor produced on expansion was used to determine if additional intermediate stages are needed. Alternatively, Townsend and Linnhoff (1983) introduced a set of qualitative guidelines based on thermodynamic principles and heuristic rules for positioning heat engines and pumps for minimizing utility consumption.

The methods discussed above are quite general in applicability, however, they share the heuristic setting of the number and the temperature of intermediate stages. A novel systematic procedure to overcome this shortcoming was proposed by Shelton and Grossmann (1986). The main idea was to finely discretize the entire temperature range providing candidate temperature levels for intermediate stages. This representation was used to generate a network superstructure representation of a refrigeration system. Using this representation, the minimum cost refrigeration system synthesis problem was posed as a mixed integer linear (MILP) optimization problem. The advantage of this method is that it systematically selects the number and temperatures of the intermediate stages. However, the refrigerants and their operating ranges were prespecified and refrigeration structures such as economizers were not accounted for.

Later, Colmenares and Seider (1989) proposed a nonlinear programming approach for the synthesis of refrigeration systems that determined both the type of refrigerants and the location of the refrigeration cycles within the heat recovery network. This approach accounted for presaturators, but not for economizers. The key advantage of this model is that it did not require temperature discretization. However, this led to highly nonlinear models whose solution to optimality may be difficult to assess. Swaney (1989) proposed an extended transportation model for integrating heat engines and pumps with process heat recovery networks. The strength of the method is that optimal heat flow patterns were determined without any reference to a detailed configuration. However, refrigerants are specified beforehand and the number of intermediate stages are fixed by assuming that they are equally spaced. An elegant graphical method for optimally placing ideal heat pumps within heat recovery networks is described by A.W. Westerberg in a textbook (Biegler et al., 1997). Finally, departures from simple vapor compression cycles employing pure refrigerants included the use of refrigerant mixtures (Cheng and Mah, 1980; Paradowski and Dufresne, 1983; Kinard and Gaumer, 1973), vapor absorption cycles (Stoecker and Jones, 1982), and mechanical subcooling (Zubair, 1994). Research results based on the methods summarized above indicate that minimum cost refrigeration systems typically involve complex, counterintuitive topologies. This complexity is not an artifact of the employed modeling features and solution methods. Patented refrigeration configurations share the same complexities (Liu and Pevier, 1985; Paradowski and Leroux, 1985; Gauberthier and Paradowski, 1981). On the microscopic scale, the need to replace CFC refrigerants with environmentally benign ones of comparable performance sparked research efforts on the molecular design of refrigerant molecules (Joback and Stephanopoulos, 1989; Gani et al., 1991; Venkatasubramanian et al., 1995; Duvedi and Achenie, 1996).

Nevertheless, the present state of the art involves a gap between the refrigeration cycle synthesis and the refrigerant design or even the selection problem. Specifically, in refriger-

ation cycle synthesis the refrigerants participating in the system and their operating ranges are almost always fixed. On the other hand, in refrigerant molecule design the topology of the employed refrigeration cycle is typically somewhat simple and always prepostulated. This work attempts to narrow this gap by considering a simplified version of the problem. Instead of designing refrigerant molecules (see above paragraph), the best refrigerants are selected from a prespecified list of candidate refrigerants, while their operating ranges are identified by the optimization problem. Thus, the central objective addressed in this work is how you can simultaneously optimally synthesize refrigeration cycles and select refrigerants from a list to seamlessly match the process cooling requirements while observing tractability and providing optimality guarantees. The starting point of our developments is the generalized network representation of Shelton and Grossman (1986). This superstructure representation is extended to account for more elaborate refrigeration features and allow the automatic selection of refrigerants from a list of available ones.

Problem Definition

The problem addressed in this work is stated as follows:

Given a set of process cooling loads, heat sinks at different temperatures, and a set of available refrigerants, find the refrigeration cycle topology, operating conditions, and refrigerants that optimize a weighted sum of the investment and operating costs for the refrigeration system.

The proposed model involves a superstructure representation for both the synthesis and the refrigerant selection problems. The model allows for the identification of the number of stages, their operating temperature ranges, the type of refrigerant participating in a stage, the temperature where a switch between two refrigerants occurs, the use of economizers, presaturators, or heat exchangers between intermediate stages. The objective to be optimized considers both investment and operating costs.

The modeling features and assumptions are as follows;

- (1) Vapor compression cycles with only pure refrigerants are considered.
- (2) The condenser outlet is a saturated liquid and the evaporator outlet is a saturated vapor.
- (3) Expansion valves are treated as isoenthalpic.
- (4) Refrigerants vapor heat capacities are assumed to remain constant within a simple compression cycle, but they may change value for different cycles. Liquid heat capacities and heats of vaporization are explicitly treated as temperature-dependent.
- (5) Refrigerant switches are allowed only in the direction of decreased volatility. For example, a propane stage may follow an ethane stage but not vice versa.
- (6) The investment cost for a compressor is described with a fixed-charge term and a variable term linearly related to work input. These costing parameters are assumed to be dependent only on the compressor suction-side temperature and independent of the compression ratio.

Assumption 1 defines the scope of this work. Extensions of the work to refrigerant mixtures is currently under investigation. Assumption 2 is in-line with current industrial practice and is listed only for the sake of completeness. Assumption 3

can easily be relaxed by incorporating an efficiency factor in the energy balance equations. Moreover, a letdown turbine can be incorporated in place of an expansion valve without affecting the model structure. Assumption 4 is reasonable because the temperature range of an intermediate stage rarely exceeds 50°C over which the vapor heat capacity can be approximated with an average value. Assumption 5 restricts the direction of refrigerant switches. It is justified on the grounds that when a refrigerant rejects energy, it is advantageous to reject it to a refrigerant at a lower pressure since it has a higher latent heat of vaporization. Lower pressure is achieved by stacking the refrigerants in the refrigeration cascade in a decreasing volatility order. Finally, assumption 6 implies a fixed-charge plus linear term representation to capture economies of scale in a simple manner. Admittedly, this may be oversimplifying in some cases. More complex costing expressions utilizing piecewise linear concave expressions at the expense of additional binary variables can be incorporated in the model without affecting its special structure.

The basic features and notation of the refrigeration superstructure are described in the next section, key questions are raised, and the proposed description is clarified with a simple example.

Background and Terminology

The starting point of the proposed refrigeration system model is that proposed by Shelton and Grossmann (1986). A number of refrigeration constructs outlined in Barnes and King (1974), Cheng and Mah (1980), and Colmenares and Seider (1989) have also been incorporated. Most of the terminology introduced in previous work has been retained here.

A *simple vapor compression cycle* is composed of a condensation, expansion, evaporation, and compression step. A *multistage refrigeration system* is a series-parallel combination of simple vapor compression cycles (simple cycles or stages). In the context of a multistage system the evaporation and condensation steps of a simple cycle do not necessarily imply the presence of heat exchangers, but rather denote phase changes occurring in the refrigeration fluid. A heat exchanger is used only when heat is removed from a process stream or if a simple cycle rejects heat to another simple cycle involving a different refrigerant. If the same refrigerant operates between two adjacent simple cycles, then a presaturator or an economizer is used instead. A presaturator and an economizer are shown in Figure 1. Both of them are essentially gas-liquid separators that separate the inlet liquid-vapor mixture into saturated liquid and saturated vapor. For a presaturator, the saturated vapor is sent directly to the compressor of the stage above, whereas in the case of an economizer, the saturated vapor is mixed with superheated vapor from the compressor of the stage below and the resulting superheated vapor is sent to the compressor of the stage above. Presaturators result in higher refrigerant flow rates, while economizers yield higher inlet temperatures to the compressor. Compression costs are directly proportional to the refrigerant flow rate times the inlet temperature. Therefore, the selection between an economizer and presaturator must properly reflect this economic trade-off.

The temperature at which the (pure) refrigerant in a simple cycle evaporates or condenses is referred to as a *tempera-*

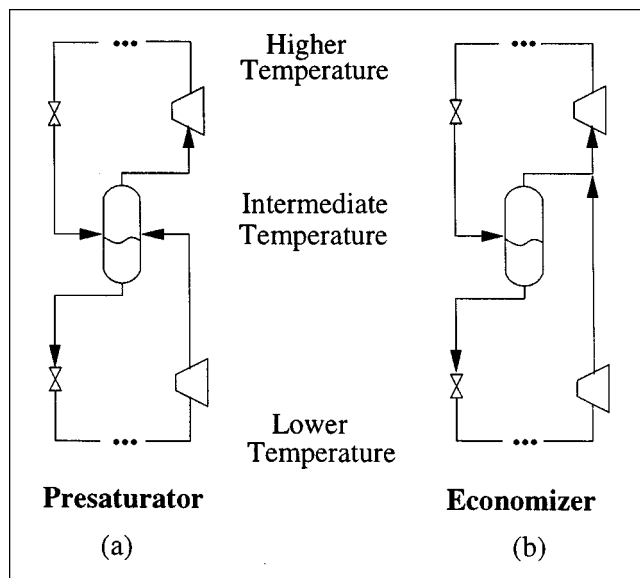


Figure 1. Presaturator and economizer configuration.

ture level. If a presaturator or an economizer is used between two simple cycles with the same refrigerant, the temperature of condensation in one cycle is equal to the evaporation temperature of the other cycle. Therefore, a presaturator or an economizer, serving as links between two simple cycles using the same refrigerant, can be described with a single temperature level. A heat exchanger, however, requires two temperature levels to model the hot stream and the cold stream. The refrigerants used in a refrigeration system are constrained by the temperature range over which they can operate. This range of temperatures is referred to as the *allowable operating temperature range* of the refrigerant. The lowest operating temperature of a refrigerant should be above the normal boiling point if vacuum conditions at the evaporator are to be avoided. The highest operating temperature is always less than the critical temperature to keep the condenser away from critical conditions.

Superstructure Description

A number of questions must be answered when synthesizing a refrigeration system:

- (1) Which refrigerants will operate in the refrigeration system?
- (2) How many stages are needed, and what should be the intermediate level temperatures?
- (3) At what temperature level should a switch from one refrigerant to another take place?
- (4) Should a presaturator, economizer, or a combination be utilized at a particular temperature level?

A superstructure-based model is proposed whose optimal solution directly answers the aforementioned questions. This superstructure superimposes all feasible and allowable refrigeration configurations and refrigerants. The superstructure description defines a hierarchy where at the top the refrigerants which may participate in the system are prepostulated. For each such refrigerant, all possible refrigeration stages (that is, number of levels and operating temperatures) are

postulated. Finally, for each stage (temperature level) all possible configurations (topologies) involving heat exchangers, economizers, and/or presaturators are constructed. The allowable refrigerants in the first level of hierarchy are specified by prepostulating a list of refrigerants that may participate in the system. The identification of the allowable cycle configurations for each refrigerant in the second level of hierarchy is performed similarly to the approach of Shelton and Grossmann (1986). Instead of treating the stage temperatures as variables (Colmenares and Seider, 1989), a discretization is employed of the temperature scale of each allowed refrigerant (Shelton and Grossmann, 1986) which provides candidate temperature levels for refrigeration stages. A simple cycle can thus operate between any pair of postulated temperature levels of the allowed refrigerant. Also, energy from a temperature level of one refrigerant can be rejected to a temperature level of another refrigerant at a lower temperature. This accounts for all possible energy flow patterns in the refrigeration system. The advantage of this approach is that nonlinearities resulting from treating temperatures as variables are avoided. The disadvantage is that a fine temperature discretization is needed to ensure that no good solutions are overlooked due to coarseness of the discretization.

A convenient way to represent the allowed energy flows in the system is through a network representation $\mathcal{G}(\mathcal{L}, \mathcal{A})$. Node set $\mathcal{L} = \{l\}$ contains all the candidate temperature levels in the refrigeration system. This set is further partitioned into the following four subsets:

- (1) $\mathcal{L}^{\text{load}}$: temperature levels corresponding to process streams to be cooled.
- (2) $\mathcal{L}^{\text{sink}}$: temperature levels corresponding to process streams to be heated.
- (3) \mathcal{L}^{cw} : refrigerant temperature levels which may reject heat to cooling water.
- (4) \mathcal{L}^{int} : refrigerant temperature levels from which heat is not rejected to cooling water.

This implies that $\mathcal{L}^{\text{int}} = \mathcal{L} \setminus \{\mathcal{L}^{\text{load}} \cup \mathcal{L}^{\text{sink}} \cup \mathcal{L}^{\text{cw}}\}$. Parameter ref_l identifies the refrigerant operating at a level l . Arc-set $\mathcal{A} = \{(l, m)\}$ denotes the set of all possible energy flows between any two temperature levels. This set is further partitioned into the following two subsets:

- (1) $\mathcal{A}_s = \{(l, m) | m \in \mathcal{L}, ref_l = ref_m, T_m > T_l\}$, which is the set of all energy flows forming a simple cycle; and
- (2) $\mathcal{A}_e = \{(l, m) | m \in \mathcal{L}, ref_l \neq ref_m, T_l \geq T_m + \Delta T_{\min}, T_l \leq T_m + \Delta T_{\max}\}$ which is the set of all energy flows representing energy transfer to or from a process stream or denoting a switch between refrigerants.

This partitioning is imposed due to the different types of energy balances required for each case. Here, ΔT_{\min} and ΔT_{\max} are the minimum and the maximum allowed approach temperature in a heat exchanger.

Finally, the lowest level of hierarchy identifies all possible configurations of each potential stage (temperature level) in the refrigeration system. The superstructure representation of a single temperature level is shown in Figure 2. This figure pictorially illustrates the superimposition of all possible process choices for node l in the network $\mathcal{G}(\mathcal{L}, \mathcal{A})$. The entire refrigeration system is thus composed of a cascade of single level superstructures linked through energy and mass flows. Level $l \in \mathcal{L}$, shown in Figure 2, superimposes heat exchanger C which accepts energy from other refrigerants/pro-

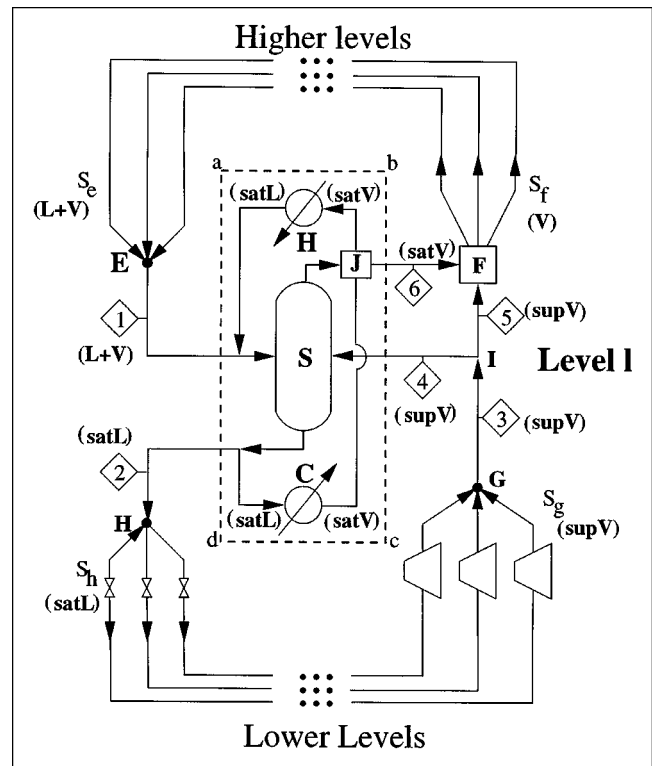


Figure 2. Single level l refrigeration superstructure.

cess streams, heat exchanger H, which rejects heat to other refrigerants/process streams, and the vapor-liquid (V-L) separator S along with all the necessary mass and energy flows. The streams constituting sets S_e and S_f correspond to arcs $(l, m) \in \mathcal{A}_s$ forming simple cycles between l and m . Similarly, the sets S_h and S_g correspond to arcs $(m, l) \in \mathcal{A}_e$ forming simple cycles between m and l . Other streams include stream 4 which enters into the V-L separator and stream 5 which bypasses the V-L separator. Block J is a junction which represents a mixing or a splitting point. Block F is a superstructure representation of the splitting and mixing of streams 5 and 6 as they form the streams of set S_f . This is shown in detail in Figure 3. The notation L, V, sat L, sat V, sup V, and L+V implying liquid, vapor, saturated liquid, saturated vapor, superheated vapor and liquid-vapor mixture, respectively, is used in Figures 2 and 3 to denote the phase of each stream. It is straightforward to show that the present configuration encompasses the presaturator and economizer configurations as special cases. Specifically, if heat exchangers C and H are absent and stream 5 has a zero flow rate, then a presaturator is recovered while a zero flow rate for stream 4 provides an economizer.

Figures 4a and 4b illustrate the superstructure representation of an evaporator and condenser, respectively. The configuration of level l when only evaporation takes place is obtained by setting the flow rates of streams 2, 3, 4, and 5 to zero (see Figure 4a). The equivalence of the configuration shown in Figure 4a with an evaporator is readily established by observing that the heat accepted by the refrigerant stream evaporates the liquid portion of the liquid-vapor mixture entering the evaporator. Therefore, the evaporation process can be

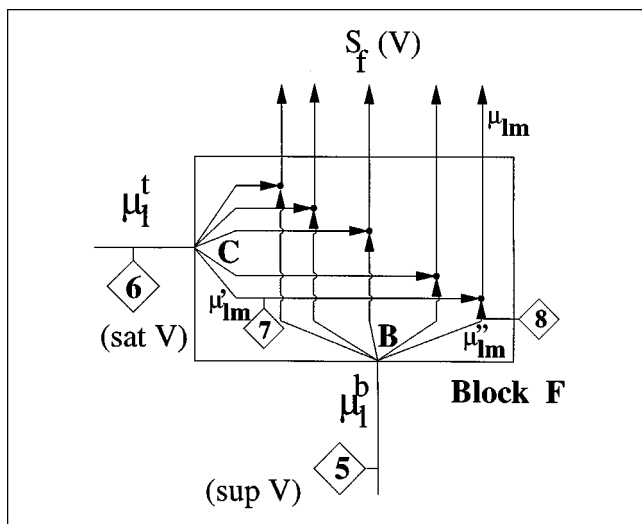


Figure 3. Superstructure of stream splitting and mixing of block F in Figure 2.

abstracted for modeling purposes as a two-step process involving, first, the separation of a liquid-vapor mixture in S and subsequent evaporation of the saturated liquid in C (Figure 4a). Similarly, the configuration of level l when only condensation occurs is obtained by setting the flow rates of streams 1, 5 and 6 to zero (Figure 4b). This corresponds to a mathematical construct which treats the condensation of the refrigerant as a two-step process in which the condensing stream indirectly rejects heat. This is accomplished by rejecting heat to an auxiliary stream 1 in the separator S. This stream in turn rejects the heat to other process streams or refrigerants through heat exchanger H (Figure 4b).

Next, a simple ethane-propane refrigeration system is considered to clarify the set definitions in the description of the superstructure. The objective here is to synthesize a refrigeration system which removes 100 kW of heat from a process stream cooling it to 190 K. Ethane and propane are the only two available refrigerants. The operating temperature range of ethane is 187 K–245 K and that of propane is 240 K–310 K truncated by the cooling water temperature (310 K). The operating range of ethane is discretized to allow for two intermediate temperature levels at 205 K and 238 K. Only one additional intermediate level at 270 K is allowed for propane. The network superstructure $\mathcal{G}(\mathcal{L}, \mathcal{A})$ for this system, shown in Figure 5, involves eight temperature levels corresponding to nodes in the graph. Based on the definitions described above, the sets used in the network representation are as follows

$$\mathcal{L} = \{1, 2, 3, 4, 5, 6, 7, 8\}$$

$$\mathcal{L}^{\text{load}} = \{1\}$$

$$\mathcal{L}^{\text{sink}} = \emptyset$$

$$\mathcal{L}^{\text{cw}} = \{8\}$$

$$\mathcal{L}^{\text{int}} = \{2, 3, 4, 5, 6, 7\}$$

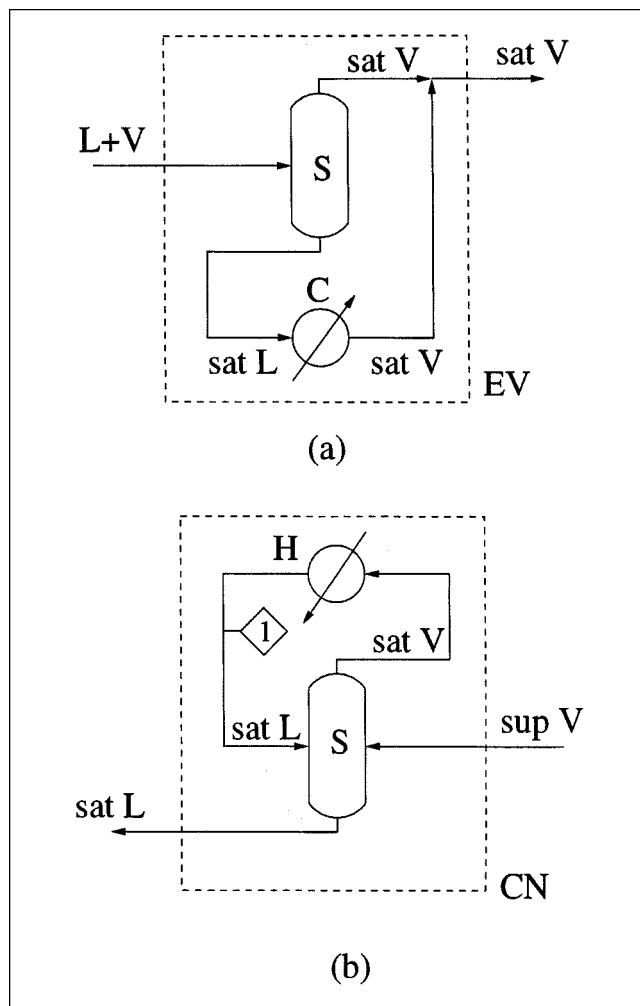


Figure 4. Single level configuration for an evaporator and condenser.

$$\mathcal{A} = \{(1, 2), (2, 3), (2, 4), (2, 5), (3, 4), (3, 5), (4, 5), (5, 6), (6, 7), (6, 8), (7, 8)\}$$

$$\mathcal{A}_r = \{(2, 3), (2, 4), (2, 5), (3, 4), (3, 5), (4, 5), (6, 7), (6, 8), (7, 8)\}$$

$$\mathcal{A}_e = \{(1, 2), (5, 6)\}$$

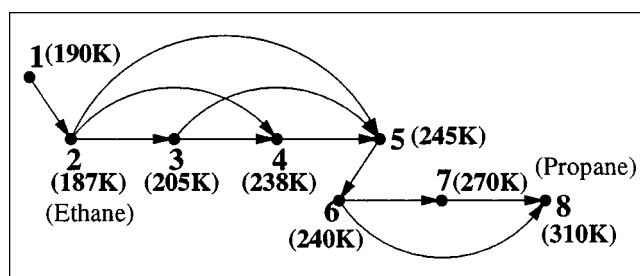


Figure 5. Network representation of ethane-propane refrigeration system.

The next section discusses how this superstructure representation is utilized within an optimization framework to solve for the optimal values of the energy flows in the network.

Model Formulation

In this section, the modeling equations which are primarily superstructure mass and energy balances are discussed. These constraints are then incorporated into the optimization formulation whose objective function minimizes the sum of investment and operating compression costs.

Mass and energy balances

A description of the streams shown in Figures 2 and 3 is provided by tracking a simple cycle between level l and a level above, as well as a simple cycle between level l and a level below. Consider first a simple cycle operating between levels l and m , where l is below m . The refrigerant operating in this simple cycle leaves level l as a saturated or superheated vapor through stream set S_f , has a molar enthalpy of h_{lm}^{out} , and a temperature of T_{lm}^{out} . It returns to level l with enthalpy h_{lm}^{in} through stream set S_e that mixes to form stream 1. Stream 1 is a vapor-liquid mixture. Next, consider a simple cycle operating between levels l and m where l is above m . The refrigerant, denoted as stream 2, leaves level l as a saturated liquid with enthalpy h_l^{liq} . Stream 2 then splits into the streams composing set S_h . It returns as a superheated vapor to level l through stream set S_g . The streams forming set S_g mix to form the superheated stream 3. This stream splits into stream 4 with a flow rate μ_l^j which enters the separator and stream 5 with a flow rate μ_l^b that bypasses the separator. Stream 6, which is the top product of the separator, is a saturated vapor with a flow rate μ_l^t and enthalpy h_l^{vap} . Afterwards, streams 5 and 6 enter the mixing/splitting block F (see Figure 3), where they combine in different proportions to form the streams composing set S_f . Specifically, the fraction of stream 5 going to level m has a flow rate of μ_{lm}'' and the fraction of stream 6 entering level m is μ_{lm}' . These two streams combine to form the refrigerant stream μ_{lm} operating in the simple cycle between levels l and m . Information

about every process stream shown in Figures 2 and 3 including phase, flow rate, temperature, and molar enthalpy is summarized in Table 1.

The mass and energy balances for a single temperature level l are discussed next. The key variables of interest are the refrigerant flow rates μ_{lm} within simple cycles operating between levels l and m , the energy D_{lm} , rejected to the simple cycle operating between levels l and m by level l , the work input W_{lm} to the simple cycle, and the enthalpies h_l^{cp} , h_{lm}^{out} . The flow rates through heat exchangers H and C are not considered explicitly, because they can be back-calculated from the heat duties. The modeling equations are mass and energy balances at various mixing and splitting points in the configuration. These include the mass and energy balance around block $abcd$ shown in Figure 2

$$\sum_{m:(l,m) \in \mathcal{A}_i} \mu_{lm} + \mu_l^j = \sum_{m:(m,l) \in \mathcal{A}_i} \mu_{ml} + \mu_l^i, \quad \forall l \in \mathcal{L}^{\text{int}} \quad (1)$$

$$\begin{aligned} & \sum_{m:(l,m) \in \mathcal{A}_i} \mu_{lm} h_{lm}^{\text{in}} + \mu_l^j h_l^{\text{cp}} + \sum_{m:(m,l) \in \mathcal{A}_e} D_{ml} \\ &= \sum_{m:(m,l) \in \mathcal{A}_i} \mu_{ml} h_l^{\text{liq}} + \mu_l^t h_l^{\text{vap}} + \sum_{m:(l,m) \in \mathcal{A}_e} D_{lm}, \quad \forall l \in \mathcal{L}^{\text{int}} \end{aligned} \quad (2)$$

Mass balances at splitters B and C (see Figure 3)

$$\mu_l^b = \sum_{m:(l,m) \in \mathcal{A}_i} \mu_{lm}'', \quad \forall l \in \mathcal{L}^{\text{int}} \quad (3)$$

$$\mu_l^t = \sum_{m:(l,m) \in \mathcal{A}_i} \mu_{lm}', \quad \forall l \in \mathcal{L}^{\text{int}} \quad (4)$$

Mass and energy balances at junction A (Figure 3)

$$\mu_{lm}' + \mu_{lm}'' = \mu_{lm}, \quad \forall (l,m) \in \mathcal{A}_i \quad (5)$$

$$\mu_{lm}' h_l^{\text{vap}} + \mu_{lm}'' h_l^{\text{cp}} = \mu_{lm} h_{lm}^{\text{out}}, \quad \forall (l,m) \in \mathcal{A}_i \quad (6)$$

Table 1. Stream Definition and Notation (Figures 2 and 3)

Stream No.	Flow Rate	Temp.	Molar Enthalpy	State
1	$\sum_{m:(l,m) \in \mathcal{A}_i} \mu_{lm}$	T_l	$\frac{\sum_{m:(l,m) \in \mathcal{A}_i} \mu_{lm} h_{lm}^{\text{in}}}{\sum_{m:(l,m) \in \mathcal{A}_i} \mu_{lm}}$	vapor + liquid
2	$\sum_{m:(m,l) \in \mathcal{A}_i} \mu_{ml}$	T_l	h_l^{liq}	saturated liquid
3	$\sum_{m:(m,l) \in \mathcal{A}_i} \mu_{ml}$	T_l^{cp}	h_l^{cp}	superheated vapor
4	μ_l^j	T_l^{cp}	h_l^{cp}	superheated vapor
5	μ_l^b	T_l^{cp}	h_l^{cp}	superheated vapor
6	μ_l^t	T_l	h_l^{vap}	saturated vapor
7	μ_{lm}'	T_l	h_l^{vap}	saturated vapor
8	μ_{lm}''	T_l^{cp}	h_l^{cp}	superheated vapor
Set S_e	μ_{lm}	T_l	h_{lm}^{in}	vapor + liquid
Set S_f	μ_{lm}	T_{lm}^{out}	h_{lm}^{out}	vapor
Set S_h	μ_{ml}	T_l	h_l^{liq}	saturated liquid

The mass balance at splitter I is not considered, because it is linearly related to the rest of the mass balances. The linking relation between the energy accepted by a simple cycle and the refrigerant flow rate is

$$D_{lm} = \mu_{lm}(h_{lm}^{\text{out}} - h_{lm}^{\text{n}}), \quad \forall (l, m) \in \mathcal{A}_i \quad (7)$$

The relation between the flow rates of all simple cycles operating between levels below l and level l and the energy rejected by them to level l is as follows

$$\sum_{m:(l, m) \in \mathcal{A}_i} (D_{ml} + W_{ml}) = \sum_{m:(l, m) \in \mathcal{A}_i} \mu_{ml}(h_l^{\text{cp}} - h_l^{\text{liq}}), \quad \forall l \in \mathcal{L}^{\text{int}} \quad (8)$$

Finally, the defining relation for the compression work assuming ideal isentropic compression (Biegler et al., 1997) is

$$W_{lm} = \mu_{lm} T_{lm}^{\text{out}} WC_{lm}, \quad \forall (l, m) \in \mathcal{A}_i \quad (9)$$

where

$$WC_{lm} = \eta R_g \left(\frac{\gamma_l}{\gamma_l - 1} \right) \left[\left(\frac{P_m}{P_l} \right)^{\frac{\gamma_l - 1}{\gamma_l}} - 1 \right]$$

and R_g is the universal gas constant.

The key shortcoming of the above description is that nonlinearities in the form of flow rate/enthalpy products are dispersed throughout the model. This adversely affects solution tractability and prohibits the setting of optimality guarantees. We propose to remedy this shortcoming by *recasting the problem so that nonlinearities appear only within a single nonlinear constraint set and then identify conditions under which this nonlinear constraint set is redundant at the optimal solution.*

The problem reformulation is accomplished by first projecting the feasible region onto the reduced space of variables D_{lm} , W_{lm} , and μ_{lm} . This set of variables unambiguously describes the energy flow interactions of a given level with the entire refrigeration superstructure. This projection reduces the total number of variables but, more importantly, after careful manipulation, “aggregates” all nonlinearities into a single constraint set. Assuming that the optimal refrigeration topology conforms to a set of requirements yet to be determined, this single remaining nonlinear constraint set is shown to be redundant at the optimal solution. Redundancy of a constraint means that the same optimal solution is obtained even after omitting this constraint. This implies that it can *a priori* be eliminated yielding a MILP representation. The details of the projection to the reduced variable set are given in Appendix A. The optimization formulation involving the reduced variable set is discussed next.

Formulation P

$$\min z = \sum_{(l, m) \in \mathcal{A}_i} [C_f y_{lm} + (C_v + C_e) W_{lm}]$$

subject to (P)

$$\begin{aligned} & \sum_{m:(l, m) \in \mathcal{A}_i} (D_{ml} + W_{ml}) + \sum_{m:(m, l) \in \mathcal{A}_e} D_{ml} \\ & = \sum_{m:(l, m) \in \mathcal{A}_i} D_{lm} + \sum_{m:(l, m) \in \mathcal{A}_e} D_{lm}, \quad \forall l \in \mathcal{L}^{\text{int}} \quad (10) \end{aligned}$$

$$\begin{aligned} & \sum_{m:(l, m) \in \mathcal{A}_i} \mu_{lm} [\Delta H_l^{\text{vap}} - c_{pl}^{\text{liq}}(T_m - T_l)] + \sum_{m:(l, m) \in \mathcal{A}_e} D_{lm} \\ & \geq \sum_{m:(m, l) \in \mathcal{A}_i} \mu_{ml} \Delta H_l^{\text{vap}} + \sum_{m:(m, l) \in \mathcal{A}_e} D_{ml}, \quad \forall l \in \mathcal{L}^{\text{int}} \quad (11) \end{aligned}$$

$$\begin{aligned} & \frac{\sum_{m:(m, l) \in \mathcal{A}_i} (D_{ml} + W_{ml})}{\sum_{m:(m, l) \in \mathcal{A}_i} \mu_{ml}} \geq \frac{D_{lm}}{\mu_{lm}} + c_{pl}^{\text{liq}}(T_m - T_l), \\ & \quad \forall (l, m) \in \mathcal{A}_i \quad (12) \end{aligned}$$

$$D_{lm} \geq \mu_{lm} [\Delta H_l^{\text{vap}} - c_{pl}^{\text{liq}}(T_m - T_l)], \quad \forall (l, m) \in \mathcal{A}_i \quad (13)$$

$$\begin{aligned} W_{lm} & = \left(\frac{WC_{lm}}{c_{pl}^{\text{vap}}} \right) [D_{lm} - \mu_{lm} (\Delta H_l^{\text{vap}} - c_{pl}^{\text{liq}}(T_m - T_l) - c_{pl}^{\text{vap}} T_l)], \\ & \quad \forall (l, m) \in \mathcal{A}_i \quad (14) \end{aligned}$$

$$Q_l^{\text{load}} = \sum_{m:(l, m) \in \mathcal{A}_e} D_{lm}, \quad \forall l \in \mathcal{L}^{\text{load}} \quad (15)$$

$$Q_l^{\text{sink}} = \sum_{m:(m, l) \in \mathcal{A}_e} D_{ml}, \quad \forall l \in \mathcal{L}^{\text{sink}} \quad (16)$$

$$D_{lm} \leq D_{lm}^U y_{lm}, \quad \forall (l, m) \in \mathcal{A}_i \quad (17)$$

$$\sum_{m:(m, l) \in \mathcal{A}_e} D_{ml} \leq \sum_{m:(l, m) \in \mathcal{A}_i} D_{lm} \quad \forall l \in \mathcal{L}' \quad (18)$$

$$\sum_{m:(l, m) \in \mathcal{A}_e} D_{lm} \leq \sum_{m:(m, l) \in \mathcal{A}_i} (D_{ml} + W_{ml}) \quad \forall l \in \mathcal{L}' \quad (19)$$

$$D_{lm}, W_{lm}, \mu_{lm} \geq 0, y_{lm} \in \{0, 1\} \quad (20)$$

The objective function is composed of the sum of the compressor investment and operating costs. Constraint set 10 is the overall energy balance for a given level. Constraint set 11 describes the energy balance around area abcd shown in Figure 2. The nonconvex constraint set 12 maintains consistency of the mass and energy balances at the mixing block F. The refrigerant stream operating in a cycle between levels l and m is formed by mixing a portion of the superheated vapor stream 5 with part of the saturated vapor stream 6 (see Figure 3). The nonconvex constraint ensures that the resulting stream from this mixing (belonging to set S_l) is less superheated than stream 5 ($h_{lm}^{\text{out}} \leq h_l^{\text{sp}}$). Inequality 13 ensures that the compressor inlet is either saturated or superheated vapor. Constraint 14 relates compression work to energy flows, temperature levels, and refrigerant mass flows. Constraint 15 ensures that the refrigeration system satisfies the cooling

loads required by the process streams. Constraint 16 maintains that the energy requirements for process streams to be heated are satisfied by the refrigeration system. Logical constraint set 17 sets the energy flow in a simple cycle to zero if the cycle does not exist. Constraints 18 and 19 ensure that consecutive refrigerant switches without a compression cycle operating between them do not occur. Finally, constraint 20 imposes the nonnegativity restriction on the variables and declares y_{lm} as binary.

Formulation (P) corresponds to a nonconvex MINLP. Nevertheless, all nonlinear terms were "isolated" within a single constraint set (Eq. 12), which safeguards against inconsistent mixing in block F. Assuming that these inconsistencies do not occur at the optimal solution after omitting constraint set 12, then a MILP problem representation can be obtained. It will be shown that if at least one of the following two properties hold at the optimal solution of the MILP, then constraint set 12 is redundant and, thus, can be eliminated.

Property 1. The destination of all energy flows emanating from level l is a single level located higher in the refrigeration structure. This property will, henceforth, be referred to as the *inverted arborescence* property in compliance with the definition of *arborescence* of a graph which implies that no two arcs enter a vertex (Minieka, 1978).

Proof. This is established by showing that the nonconvex constraint set is indirectly enforced by the other problem constraints when energy from a given level l is rejected to only one level (say n) through a simple cycle between l and n (that is, $(l, n) \in \mathcal{A}_e$). Figure 6 shows the inverted tree-like structure of a refrigeration graph conforming with Property 1. In this case, relations 10 and 11 become

$$D_{ln} = \sum_{m:(m,l) \in \mathcal{A}_i} (D_{ml} + W_{ml}) + \sum_{m:(m,l) \in \mathcal{A}_e} D_{ml} \quad (21)$$

$$\begin{aligned} & \mu_{ln} [\Delta H_l^{\text{vap}} - c_{pl}^{\text{liq}}(T_n - T_l)] \\ & \geq \sum_{m:(m,l) \in \mathcal{A}_i} \mu_{ml} \Delta H_l^{\text{vap}} + \sum_{m:(m,l) \in \mathcal{A}_e} D_{ml} \quad (22) \end{aligned}$$

It is clear from Eq. 22 that $\mu_{ln} \geq \sum_{m:(m,l) \in \mathcal{A}_i} \mu_{ml}$. Because the outlet streams from the compressors are superheated, it follows that

$$\frac{\sum_{m:(m,l) \in \mathcal{A}_i} (D_{ml} + W_{ml})}{\sum_{m:(m,l) \in \mathcal{A}_i} \mu_{ml}} \geq \Delta H_l^{\text{vap}} \quad (23)$$

It will be shown that Eqs. 21 and 22 imply the nonconvex constraint. Substituting for $\sum_{m:(m,l) \in \mathcal{A}_e} D_{ml}$ in Eq. 22 using Eq. 21 gives

$$\begin{aligned} & \mu_{ln} [\Delta H_l^{\text{vap}} - c_{pl}^{\text{liq}}(T_n - T_l)] \\ & \geq \sum_{m:(m,l) \in \mathcal{A}_i} \mu_{ml} \Delta H_l^{\text{vap}} + D_{ln} - \sum_{m:(m,l) \in \mathcal{A}_i} (D_{ml} + W_{ml}) \end{aligned}$$

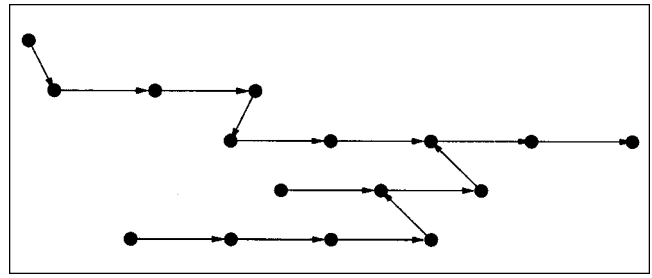


Figure 6. Inverted arborescence network structure.

which upon rearrangement results in

$$\begin{aligned} & \sum_{m:(m,l) \in \mathcal{A}_i} (D_{ml} + W_{ml}) + \Delta H_l^{\text{vap}} \left(\mu_{ln} - \sum_{m:(m,l) \in \mathcal{A}_i} \mu_{ml} \right) \\ & \geq D_{ln} + \mu_{ln} c_{pl}^{\text{liq}}(T_n - T_l) \end{aligned}$$

Utilizing Eq. 23 and the fact that $\mu_{ln} \geq \sum_{m:(m,l) \in \mathcal{A}_i} \mu_{ml}$, the above equation can be transformed to

$$\mu_{ln} \frac{\sum_{m:(m,l) \in \mathcal{A}_i} (D_{ml} + W_{ml})}{\sum_{m:(m,l) \in \mathcal{A}_i} \mu_{ml}} \geq D_{ln} + \mu_{ln} c_{pl}^{\text{liq}}(T_n - T_l)$$

Dividing this by μ_{ln} gives the nonconvex constraint 12. Therefore, the nonconvex constraint is redundant when energy from a given level is rejected to only a single level (inverted arborescence property).

Property 2. The optimal solution of formulation P does not include any economizers.

Proof. If the optimal solution does not involve any economizers, then stream 5 does not exist and the vapor stream leaving level l is simply the vapor product from the V-L separator which is saturated. Therefore, its specific enthalpy $h_l^{\text{vap}} = h_{lm}^{\text{out}}$ is less than the enthalpy h_l^{cp} of the superheated stream 3.

Satisfaction of either of these two (not mutually exclusive) properties of the optimal solution imply redundancy of the nonconvex constraint set. The next step is to, without solving formulation P, identify *a priori* whether the optimal solution will satisfy either Property 1 or 2. When the postulated refrigeration superstructure conforms to the following condition, both properties 1 and 2 hold at the optimal solution.

Condition 1. No economizers, multiple cooling loads, and a single heat sink (such as cooling water).

Clearly, condition 1 implies property 2 because the postulated superstructure does not have any economizers. The result that condition 1 implies property 1 is shown in Appendix B for the case of general concave cost functions. While it is not formally proven, computational experience indicates that Property 1 also holds for refrigeration systems involving economizers and presaturators serving multiple cooling loads with a single condenser. Property 1, however, is typically vio-

lated when multiple sinks are present. At a later section, an iterative procedure is discussed for remedying this problem. Summarizing, in this section it was shown how the original MINLP representation is equivalently transformed into an MILP problem by first isolating all nonlinearities into a single constraint set through variable projection and subsequently identifying conditions which imply redundancy for the remaining nonconvex constraint set. The next section describes additional modeling enhancements, which further improve tractability.

Modeling Improvements for Tractability

In the previous section it was shown how an MILP representation for formulation P is obtained. Fine discretizations of large-scale refrigeration problems yield hundreds of temperature levels requiring a prohibitively large number of binary variables y_{lm} . Therefore, in addition to the elimination of nonlinearities, additional modeling improvements are needed for tractability. Specifically, the following avenues are explored:

- (1) Elimination of interlevel binary variables y_{lm} .
- (2) *A priori* selection between a presaturator or economizer
- (3) Identification of tight bounds on the energy flows.

Level-to-level binary variable elimination

Property 1 not only allows the elimination of the nonconvex constraints, but also alludes to the possibility of significantly reducing the total number of binary variables. Specifically, because Property 1 disallows multiple energy flows leaving a level, level to level binary variables y_{lm} are not necessary. Instead, fewer z_l binary variables modeling activity/inactivity of a particular level suffice to describe the refrigeration superstructure. This is possible (see assumption 6) if the fixed-charge term of the compressor receiving refrigerant flow from level l is independent of the level that it is discharging to. In other words, the fixed-charge term is independent of the compression ratio for a given level. This greatly reduces the complexity of the superstructure description requiring only order N rather than order N^2 binary variables, where N is the total number of levels.

This binary variable condensation yields formulation (P_z) which differs from P only in the form of the objective function and logical constraints. The objective function is rewritten as

$$\min z = \sum_{l \in \mathcal{L}^{\text{int}}} C_f z_l + \sum_{(l,m) \in \mathcal{G}_i} (C_v + C_e) W_{lm}$$

The new logical constraints are

$$\sum_{m:(l,m) \in \mathcal{G}_i} D_{lm} \leq D_l^{\text{max}} z_l \quad \forall l \in \mathcal{L}^{\text{int}}$$

$$\sum_{m:(l,m) \in \mathcal{G}_i} D_{lm} \geq D_l^{\text{min}} z_l \quad \forall l \in \mathcal{L}^{\text{int}}$$

where D_l^{min} , D_l^{max} are lower and upper bounds, respectively, on the energy flow entering level l . Systematic ways for evalu-

ating these lower and upper bounds are discussed in a later subsection.

If Conditions 1 is not met, then Property 1 may not be satisfied. However, even in this case, formulation P_z can still be employed providing upper and lower bounds to the solution of the original formulation P (see Appendix C). This lower bounding of the optimal solution of P by P_z motivates the development of an exact iterative procedure for solving P . The basic idea is at each iteration to add the y_{lm} variables for levels which violate Property 1 in the previous iterations. The procedure terminates when the objective value in the current iteration matches the objective value in the P formulation. The details of this procedure and proof of convergence are given in Appendix C. Typically, no more than six iterations are needed for convergence.

A-priori selection between presaturator and economizer

Based on monotonicity principles, a procedure is developed for the *a-priori* selection between a presaturator and economizer for a cycle operating between level l and m (if active), before the solution of the problem. This significantly reduces the total number of variables and allows the derivation of tighter bounds for those that remain. Consider the expression for the compression work between levels l and m

$$W_{lm} = \left(\frac{WC_{lm}}{c_{p_l}^{\text{vap}}} \right) \left[D_{lm} - \mu_{lm} (\Delta H_l^{\text{vap}} - c_{p_l}^{\text{liq}} (T_m - T_l) - c_{p_l}^{\text{vap}} T_l) \right]$$

For a given amount of energy D_{lm} , the sign of the coefficient of μ_{lm} determines whether the flow rate μ_{lm} must increase or decrease to reduce the compression work W_{lm} . Therefore, the key parameter in this expression is crit_{lm} defined as

$$\text{crit}_{lm} = \Delta H_l^{\text{vap}} - c_{p_l}^{\text{liq}} (T_m - T_l) - c_{p_l}^{\text{vap}} T_l$$

Based on this parameter set, \mathcal{G}_i is further partitioned into sets \mathcal{G}_i^+ and \mathcal{G}_i^- as follows

$$\mathcal{G}_i^+ = \{ (l, m) | (l, m) \in \mathcal{G}_i, \text{crit}_{lm} \geq 0 \}$$

$$\mathcal{G}_i^- = \{ (l, m) | (l, m) \in \mathcal{G}_i, \text{crit}_{lm} < 0 \}$$

If $\text{crit}_{lm} \geq 0$, then reduction of W_{lm} is achieved when μ_{lm} increases. The maximum possible increase for μ_{lm} is dictated by constraint

$$D_{lm} \geq \mu_{lm} \left[\Delta H_l^{\text{vap}} - c_{p_l}^{\text{liq}} (T_m - T_l) \right]$$

For a given D_{lm} , the maximum value for μ_{lm} is

$$\frac{D_{lm}}{\left[\Delta H_l^{\text{vap}} - c_{p_l}^{\text{liq}} (T_m - T_l) \right]}$$

This maximum value is reached when the constraint is active. This corresponds to saturated vapor leaving level l implying that a presaturator is present at level l .

If $\text{crit}_{lm} < 0$, then reduction of W_{lm} requires decrease of μ_{lm} . The extent of this reduction in μ_{lm} is bounded by the

following constraint

$$\mu_{lm} [\Delta H_l^{\text{vap}} - c_{p_l}^{\text{liq}}(T_m - T_l)] \geq \sum_{m:(l,m) \in \mathcal{G}_i} \mu_{ml} \Delta H_l^{\text{vap}} + \sum_{m:(m,l) \in \mathcal{G}_e} D_{ml}$$

This relation corresponds to constraint 11 when level l gives heat to only one level m . The value of μ_{lm} can be reduced until this relation is satisfied as an equality. This corresponds to $\mu_l^j = 0$ (see Appendix A), which implies the presence of an economizer.

Based on simple monotonicity principles, it is determined that a presaturator must be present when crit_{lm} is nonnegative and an economizer when it is negative. Note that this analysis is performed by using only "local" information around level l . Due to synergistic effects between different levels, it is possible that these results might be invalidated even though we were unable to produce a counterexample. Note that a parameter similar to crit_{lm} was also employed by Barnes and King (1974). The consequence of this analysis is that both μ_{lm} and W_{lm} can be expressed as a function of D_{lm} and, thus, be eliminated for $[(l, m) \in \mathcal{G}_i^+]$. Because crit_{lm} is much more likely to be positive than negative, the aforementioned variable elimination scheme causes a significant reduction in the total number of variables in the formulation.

Derivation of tight bounds on the energy flows

The derivation of tight bounds for the energy flows is important because they determine the tightness of the LP relaxation of the MILP formulations. A procedure for obtaining tight bounds based on graph theory is described below.

Consider a single load Q^{load} at level 1 and an arbitrary path \mathcal{P}_l from node 1 to node l . Let the path consist of m nodes denoted by p_i , $i = 1, 2, \dots, m$ where $p_1 = 1$ and $p_m = l$. The path can be represented using the arcs of the graph which form the path

$$\mathcal{P}_l = \{(1, p_2), (p_2, p_3), \dots, (p_{i-1}, p_i), \dots, (p_{m-1}, l)\}$$

If w_{lm} is the work required to pump a unit of energy from level l to level m , the amount of energy reaching each one of the nodes p_i is

$$\begin{aligned} Q_1 &= Q^{\text{load}} \\ Q_{p_2} &= Q_1 + W_{1p_2} = Q^{\text{load}}(1 + w_{1p_2}) \\ Q_{p_3} &= Q_{p_2} + W_{p_2p_3} = Q_{p_2}(1 + w_{p_2p_3}) = Q^{\text{load}}(1 + w_{1p_2})(1 + w_{p_2p_3}) \\ &\vdots \\ Q_l &= Q^{\text{load}}(1 + w_{1p_2})(1 + w_{p_2p_3}) \dots (1 + w_{p_{i-1}p_i}) \dots (1 + w_{p_{m-1}l}) \end{aligned}$$

Therefore, the amount of energy reaching level l through an arbitrary path \mathcal{P}_l in $\mathcal{G}(\mathcal{L}, \mathcal{A})$ is equal to

$$Q^{\text{load}} \prod_{(l,m) \in \mathcal{P}_l} (1 + w_{lm})$$

where w_{lm} is the work needed to pump one unit of heat from level l to level m . Let w_{lm}^L and w_{lm}^U be the minimum and maximum values of w_{lm} . D_l^{max} can be calculated by finding the path \mathcal{P}_l which maximizes

$$Q^{\text{load}} \prod_{(l,m) \in \mathcal{P}_l} (1 + w_{lm}^U)$$

This is equivalent with maximizing the logarithm of the above expression

$$\max_{\mathcal{P}_l} \sum_{(l,m) \in \mathcal{P}_l} \ln(1 + w_{lm}^U)$$

This last relation implies that finding D_l^{max} is equivalent with finding the longest path from node 1 to node l in $\mathcal{G}(\mathcal{L}, \mathcal{A})$ given that the cost of using an arc (l, m) is $\ln(1 + w_{lm}^U)$. Similarly, D_l^{min} can be obtained by finding the shortest path between node 1 and node l given that the arc costs are equal to $\ln(1 + w_{lm}^L)$. Estimates for w_{lm}^U and w_{lm}^L can be directly obtained from the expressions for W_{lm} derived previously for the presaturator and economizer case

$$w_{lm} = \frac{WC_{lm}T_l}{[\Delta H_l^{\text{vap}} - c_{p_l}^{\text{liq}}(T_m - T_l)]}, \quad \forall (l, m) \in \mathcal{G}_i^+$$

$$w_{lm} = \left(\frac{WC_{lm}}{c_{p_l}^{\text{vap}}} \right) \left[1 - \frac{\mu_{lm}}{D_{lm}} (\Delta H_l^{\text{vap}} - c_{p_l}^{\text{liq}}(T_m - T_l) - c_{p_l}^{\text{vap}}T_l) \right], \quad \forall (l, m) \in \mathcal{G}_i^-$$

Clearly, since w_{lm} is constant when a presaturator is imposed, it follows that

$$w_{lm} = w_{lm}^L = w_{lm}^U = \frac{WC_{lm}T_l}{[\Delta H_l^{\text{vap}} - c_{p_l}^{\text{liq}}(T_m - T_l)]}, \quad \forall (l, m) \in \mathcal{G}_i^+$$

In the case of an economizer, based on the previously discussed lower and upper bounds of μ_{lm} , it can be shown that

$$w_{lm}^L = \frac{WC_{lm}}{c_{p_l}^{\text{vap}}} \quad \forall (l, m) \in \mathcal{G}_i^-$$

$$w_{lm}^U = \frac{WC_{lm}T_l}{[\Delta H_l^{\text{vap}} - c_{p_l}^{\text{liq}}(T_m - T_l)]} \quad \forall (l, m) \in \mathcal{G}_i^-$$

A procedure for solving the longest and shortest path problems is described in detail in Appendix D. This analysis holds even for multiple cooling loads.

Next, three example problems of increasing difficulty are presented to illustrate the value of the proposed framework. The first example revisits the refrigeration graph discussed in the section addressing the superstructure development. It demonstrates that significant savings can be realized by systematically selecting the number and temperature of intermediate stages, considering refrigeration features such as economizers, and allowing for the automatic selection of refrigerant switch temperatures. The second example, involving

ten candidate refrigerants and four cooling loads, highlights the importance of performing the synthesis and refrigerant selection problem simultaneously rather than one after the other. Finally, the third example shows how the present framework can be integrated with heat recovery networks.

Example 1: Ethane-Propane Refrigeration System

The proposed methodology is illustrated by revisiting the ethane-propane refrigeration system addressed earlier. The cooling duty for the process stream is 100 kW. The network superstructure of the refrigeration system is shown in Figure 5. The objective here is to find the minimum cost configuration from the network superstructure described above. The main features of the methodology illustrated in this example are: (i) the automatic selection of temperature levels from the candidate levels; (ii) systematic identification of the presence of presaturator or an economizer at each level; (iii) determination of the temperature at which refrigerant switches occur; (iv) investigation of the performance of the formulation for fine temperature discretizations.

The values for C_f , C_v , and C_e used are \$2824.8/yr, \$831.67/kW yr and \$608.33/kW yr (Shelton and Grossman, 1986), respectively. The property data for the refrigerants used in all the examples are obtained from Daubert and Danner (1989). Compression is assumed to be isentropic with $\gamma_1 = 1.4$. The MILP formulations in this and subsequent examples have been solved using GAMS/CPLEX (Brooke et al., 1988) on an IBM RS6000 43P-133 workstation using a relative convergence tolerance of 1%. The refrigeration system generated by solving the MILP formulation P_z has a cost of \$220,321/yr (see Figure 7). In comparison, the straightforward configuration involving a single refrigeration stage for each refrigerant costs \$268,718/yr (22% costlier than the optimal configuration). If the economizer option is not exercised and only presaturators are allowed, the optimal configuration

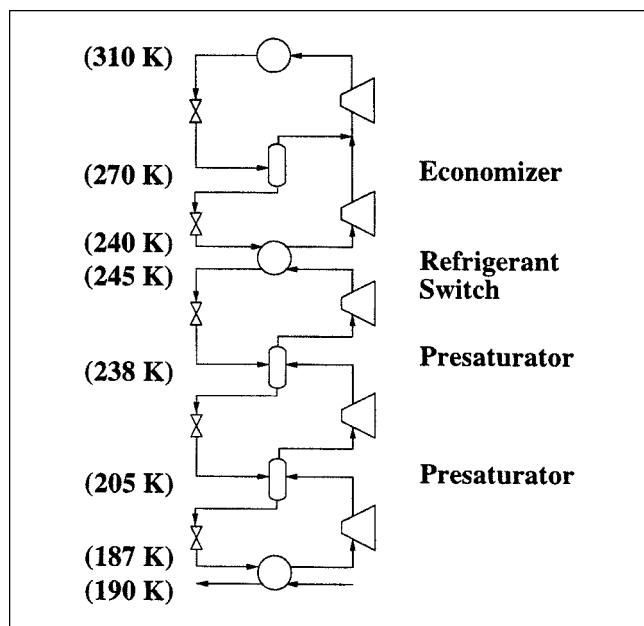


Figure 7. Minimum cost refrigeration system for Example 1 when refrigerant switch is not flexible.

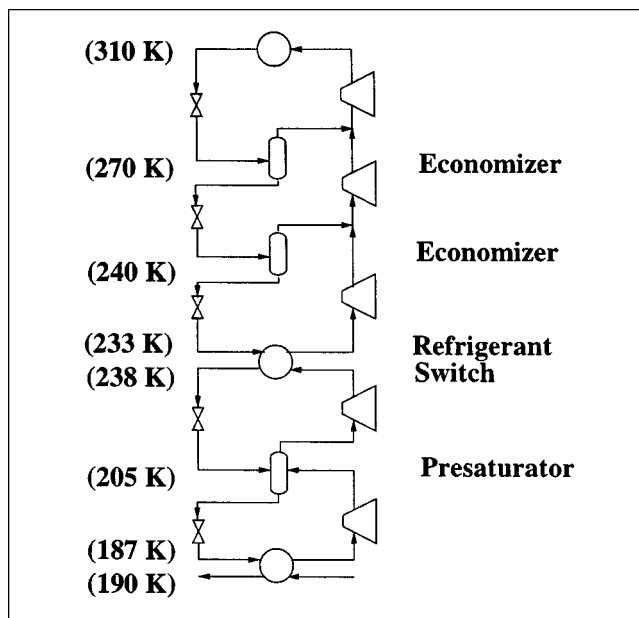


Figure 8. Minimum cost configuration for Example 1 allowing for flexibility in refrigerant switches.

involves a higher cost of \$222,562/yr. These results indicate that detailed modeling features are necessary to explore if efficient refrigeration systems are to be found.

Apart from detailed modeling features (that is, multiple stages, economizers, and so on), it is important to ensure flexibility in choosing the temperature level where refrigerant switches occur. This is highlighted by introducing additional candidate levels at 240 K and 242 K for ethane and at 233 K, 235 K, and 237 K for propane. The new superstructure consists of 13 candidate temperature levels, four possible refrigerant switches, and as many as 35 possible energy flows. The added flexibility of choosing the place where refrigerant switches occur results in an improved refrigeration configuration with a cost of \$217,693/yr. In this configuration the refrigerant switch occurs at 238 K (ethane), and an additional economizer is added in the propane system, while a presaturator is eliminated from the ethane system maintaining the same number of stages in the system (see Figure 8).

Finally, the effect of the fine discretization on the refrigeration configuration cost as well as computational requirements is examined. The full operating range for ethane (186 K–274 K) and propane (232 K–310 K) is considered and a 1 K discretization scheme is employed yielding 169 levels. The overlap in the operating temperature range of the refrigerants is 42 K (between 232 K and 274 K). The 1 K discretization yields 38 possible temperatures where the refrigerant switch may occur. The MILP formulation is solved in about 32 CPU s and the resulting configuration is shown in Figure 9. In the optimal configuration the refrigerant switch occurs at 236 K (Ethane). It involves a cost of \$207,940/yr which is 5.6% less than that with the coarser discretization. Note that, in all cases, a relatively large number of intermediate levels arise at the optimal solution. This is due to the rather conservative investment cost coefficients.

Next, the thermodynamic efficiency of the obtained optimal configuration is assessed and compared with an ideal cy-

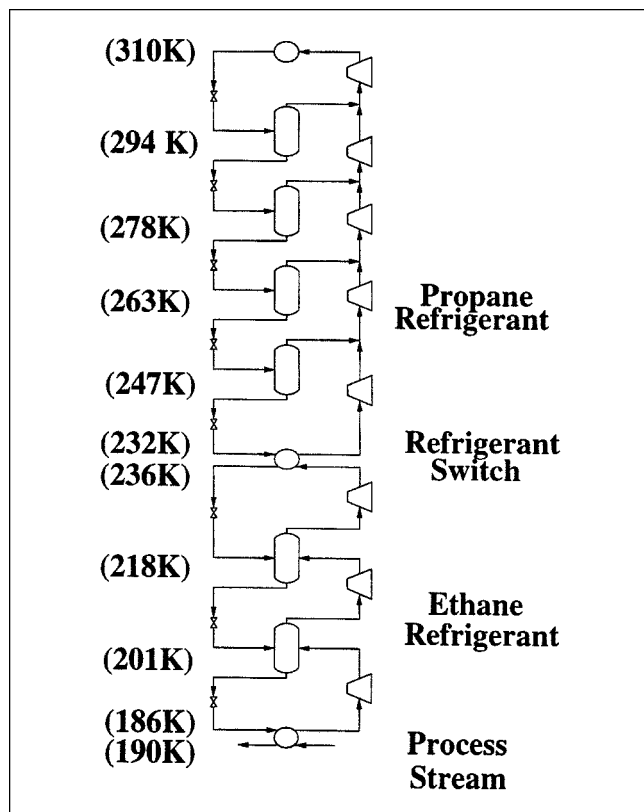


Figure 9. Minimum cost network structure for Example 1 using 1 K discretization.

cle operating between temperatures 190 K and 310 K. The minimum cost solution involves a total work input of 128.72 kW. Therefore, the coefficient of performance (COP) of the system, which is the ratio of energy intake from process stream to the work input into the system, is equal to 0.777. The thermodynamic limit given by the COP of an ideal refrigeration cycle operating between temperatures $T_1 = 190$ K and $T_2 = 310$ K is $T_1/(T_2 - T_1) = 1.583$. This apparent thermodynamic inefficiency of the optimal configuration arises, because the refrigeration system operates with real working fluids. The effect of real working fluid on COP is illustrated in Shelton and Grossman (1985), where the COP of a real refrigeration system is computed to be the difference between the ideal COP and a term which depends on the particular working fluid

$$\text{COP} = \frac{T_1}{T_2 - T_1} - \frac{c_p^{\text{liq}} T_1}{\Delta H^{\text{vap}}(T_1)}$$

The values for the second term for the refrigerants listed in Shelton and Grossmann (1985) are of order one, which implies that a real working fluid causes a significant departure of the COP from the ideal value, especially if the temperature range of operation is high. Nevertheless, the problem of finding the configuration with the highest COP can be handled by the proposed framework by minimizing the total work input into the system which amounts to solving a linear optimization program. For example 1, the maximum COP ob-

tained is 0.853, which is somewhat higher than the value of 0.777 obtained for the optimal solution. The disadvantage of using COP as the objective function is that it does not take into account the investment cost associated with the compressors and, therefore, typically results in a configuration featuring a very large number of intermediate stages.

In summary, this example demonstrates that, even for simple refrigeration problems, significant cost savings are attainable over intuitive solutions based on the proposed superstructure. In this example the optimal refrigeration system involved both prepostulated refrigerants. Identifying the optimal subset of refrigerants to be employed from a larger set of available ones is addressed in the next example. In addition, the effect of multiple cooling loads is examined.

Example 2: Multiple Cooling Loads

This example explores the use of the proposed methodology for synthesizing optimal refrigeration systems when multiple loads are present and refrigerants are selected from an extensive list. The refrigerants are grouped together in blocks of decreasing volatility as shown in Figure 10. Refrigerants within a block have similar volatilities and refrigerant switches are allowed only from a block of refrigerants with higher volatility to a block of refrigerants with lower volatility (see Assumption 5). The investment cost coefficients are obtained by performing a least-squares fit of the fixed-charge plus linear term on Guthrie's cost correlation (Douglas, 1988), converted to 1998 using the M&S Index. The fixed-charge and variable cost values are respectively $C_f = \$91,925.66/\text{yr}$ and $C_v = \$165.20/\text{kW yr}$. The compressors are assumed to be driven by electric motors [electricity unit cost $C_e = \$525.60/\text{kW yr}$ (Turton et al., 1998)]. The investment cost is annualized with a coefficient of 10%.

The objective here is to refrigerate four process streams whose temperatures and cooling loads are given in Table 2. Four different levels of discretization (that is, 8 K, 4 K, 2 K, and 1 K) are considered to study the effect of discretization on the trade-off between accuracy vs. computational requirements. Table 3 summarizes the total number of levels, opti-

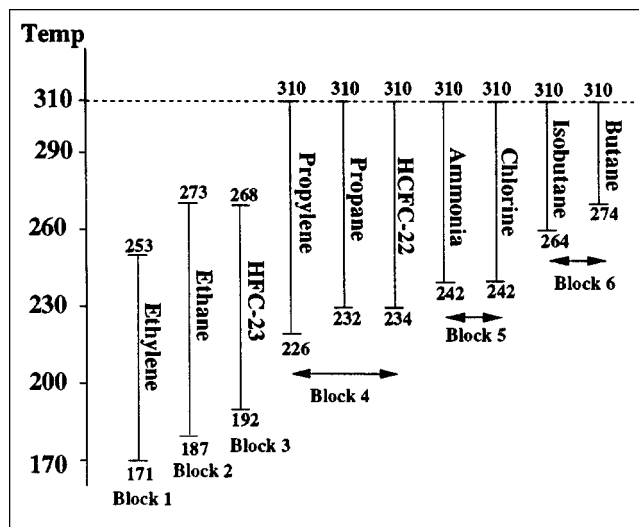


Figure 10. Refrigerant blocks for Example 2.

Table 2. Temperature and Cooling Loads of Process Streams for Example 2

No.	Cooling Load (kW)	Temperature (K)
1	100	175
2	300	200
3	150	230
4	200	245

mal refrigeration system cost, relative gap between upper and lower bound for the MILP, and CPU times for the four different cases. Finer discretizations, as expected, by providing more choices for intermediate levels, result in improved objective function values. However, this improvement comes at the expense of a significant increase in the CPU requirements. In fact, case 4 (1 K discretization) does not meet the imposed 1% relative convergence tolerance even after 10,000 s.

The network representation of the optimal solutions for the four cases are shown in Figure 11. In these diagrams, dots represent temperature levels, temperature is increasing from left to right, and levels corresponding to the same refrigerant form a horizontal line. The optimal solution for the 8 K case involves refrigerants ethane, ethylene, and propylene operating in seven stages and featuring two economizers in the propylene section. Both 4 K and 2 K cases (as well as the incomplete solution for the 1 K case) involve five stages and refrigerants ethylene, propylene, and chlorine operating with only presaturators. Note that even though ten refrigerants can potentially participate in the system, the optimal solution involves only three refrigerants. The topology of the refrigeration system for the 8 K case is considerably different than that of the 4 K case. In contrast, the topology for the 4 K case is identical with that of the 2 K case with only minor differences in the location of the intermediate levels. The structural evolution of the optimal solution as finer discretization schemes are employed suggests the following conjecture. *For every problem, there is a discretization level past which any finer discretizations cause no structural modifications in the optimal solutions and the only changes are slight differences (fine-tuning) in the temperature of the active levels.*

This conjecture along with the increased computational requirements motivates the development of a local search procedure [that is, LSP(δn)] which utilizes information from the optimal solution of the previous discretization level to constrain the search when a finer discretization is imposed. The LSP reduced superstructure is formed by the levels which were active at the optimal solution of P_z plus δn levels before and after each active level. Typically, a small value of δn

Table 3. Computational Performance of Different Discretizations for Example 2

No.	Total Levels	Cost (\$/yr)	Rel. Gap (%)	CPU (s)
8 K	96	1,200,084	0.98	8.33
4 K	187	996,528	0.92	18.23
2 K	364	984,187	1.00	796.91
1 K	714	982,448	5.12	10^4

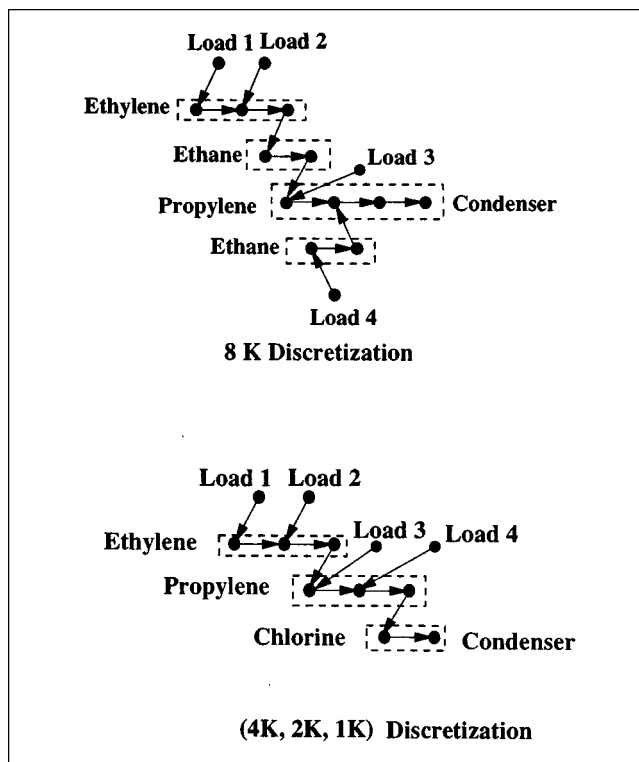


Figure 11. Optimal network topology for different discretizations of Example 2.

is used to ensure fast computation times ($\delta n = 1$ for this example). This procedure is repeated until the same solution is obtained for two consecutive iterations. By applying this local search procedure for the 1 K case, a refrigeration configuration is found whose cost is \$971,908/yr (see Figure 12). This is about 1.2% less than the solution for the 2 K case.

Next, a comparison is made between the solution obtained from the current formulation for the 2 K discretization and a solution in which the participating refrigerants are selected beforehand based on the heuristic rule of Cheng and Mah (1980). This comparison is performed for different allowable minimum approach temperatures ΔT_{min} in the heat exchangers. This heuristic primarily relies on using refrigerants with lower pressure so that the latent heat of vaporization is high and also tries to minimize the number of refrigerants used. First, the refrigerants, whose normal boiling point is near the coldest load temperature, are identified. In this case, ethylene is the only candidate which can satisfy cooling load 1 and, hence, is selected to participate in the system. Since the operating temperature range of ethylene is 171 K–253 K, it can be used to satisfy the cooling requirements for the remaining loads. The energy rejected from the ethylene system needs to be removed by another refrigerant. Again, a refrigerant with the highest boiling point that can receive this energy is chosen. In this case, a choice must be made between ammonia and chlorine, both of which can operate up to 310 K. Therefore, the comparison of the present formulation is made with two cases, one in which the refrigerants are ethylene and ammonia, and other in which they are ethylene and chlorine. The results are summarized in Table 4. The table

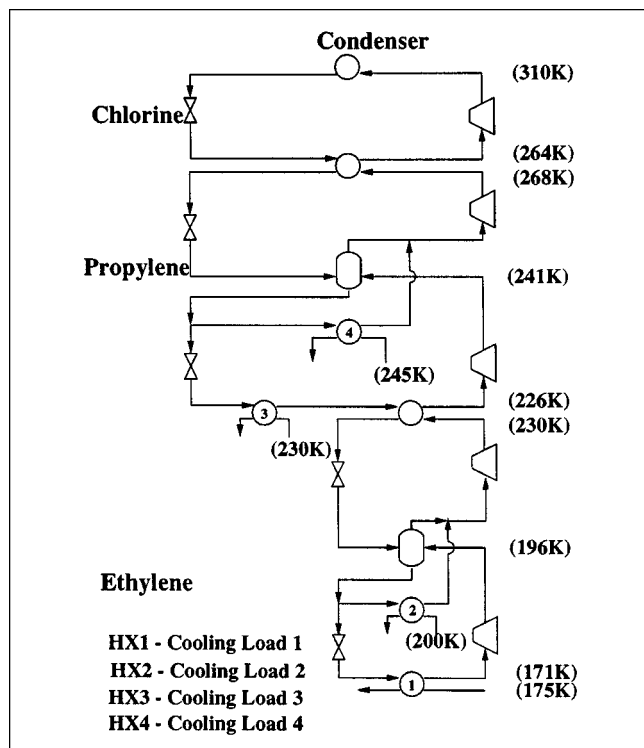


Figure 12. Minimum cost refrigeration structure for Example 2 using local search.

shows that the heuristic coincidentally works well for $\Delta T_{\min} = 3$ K, but it is much less successful for $\Delta T_{\min} = 2$ K and $\Delta T_{\min} = 4$ K. These results of varying success for the heuristic clearly justify the need to perform refrigeration cycle synthesis and refrigerant selection simultaneously in a unified framework.

In summary, this example reveals that complex, nonintuitive optimal topologies could be generated by the proposed methodology. In addition, increased CPU requirements and the lack of apparent structural modifications in the optimal solution motivate the use of a local search procedure (that is, LSP) to guide fine discretizations. The next example addresses how the proposed framework handles integration of the refrigeration system with a process heat recovery network implying not only multiple cooling loads but also multiple sinks.

Table 4. Heuristic Refrigerant vs. Optimal Refrigerant

ΔT_{\min}	Refrigerants	Cost (z \$/yr)	$\frac{z(\text{heuristic}) - z(\text{optimal})}{z(\text{optimal})}$
2 K	optimal	919,278	—
2 K	Ethylene, Chlorine	947,927	3.1
2 K	Ethylene, Ammonia	959,142	4.3
3 K	optimal	941,123	—
3 K	Ethylene, Chlorine	943,355	0.2
3 K	Ethylene, Ammonia	954,519	1.4
4 K	optimal	984,187	—
4 K	Ethylene, Chlorine	1,068,083	8.5
4 K	Ethylene, Ammonia	1,078,317	9.6

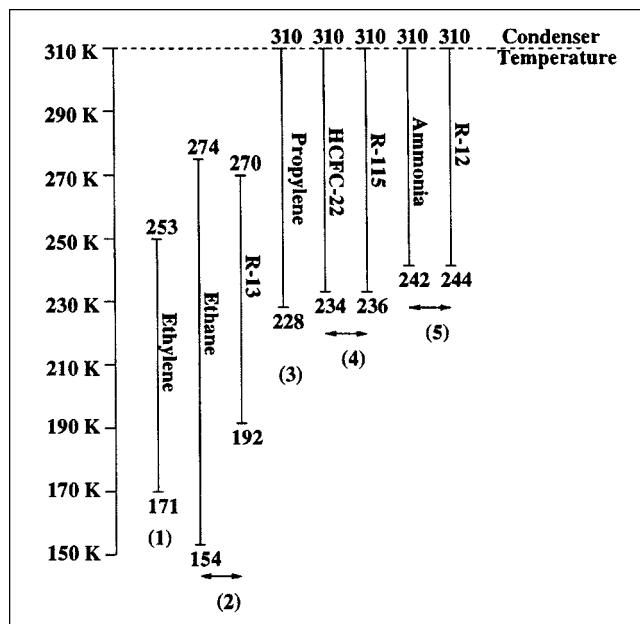


Figure 13. Refrigerant blocks for Example 3.

Example 3: Integration with a Heat Recovery Network

This example highlights the proposed methodology for the case of multiple heat sinks that typically arise when a refrigeration system is integrated with the process heat recovery network. It is a modified version of the problem addressed by Colmenares and Seider (1989) that involves synthesizing a cascade refrigeration system integrated with a heat recovery system to satisfy the heating and cooling demands for an ethylene plant separation train. The eight refrigerants employed in this example and their operating temperature ranges are shown in Figure 13. The objective function in this example also includes cooling water costs in addition to the investment and operating costs of the compressor. Another departure from previous examples is that the lowest adopted operating temperature of ethane (154 K) (Colmenares and Seider, 1989) is well below its normal boiling point at 184.5 K. Cost parameters, obtained from Colmenares and Seider (1989), are listed in Table 5. The fixed-charge and variable cost term for the compressor investment cost are obtained, as in the previous example, by performing a least-squares fit on the concave cost expressions.

The temperature interval diagram established by Colmenares and Seider (1989) is shown in Figure 14. Temperatures (cold temp. scale, $\Delta T_{\min} = 10$ K) in that diagram denote cold and hot process stream inlet and outlet temperatures.

Table 5. Cost Related Parameters for Example 3

Investment cost	1,925 $W^{0.963}$
Fixed Charge (C_f)	\$21,582/yr
Variable Charge (C_v)	\$205/kW·yr
Cost of Electricity	\$0.04/kW·h
Cost of Cooling Water	\$0.07/1,000 gal
Return of Investment	15%

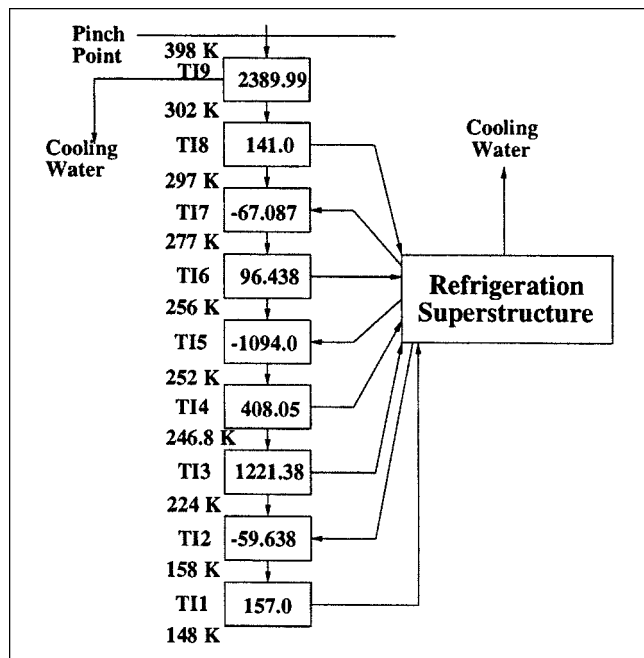


Figure 14. Temperature interval diagram for Example 3.

Energy entries within boxes denote the energy surplus or deficit for each temperature interval in kW. Temperature intervals with a heat surplus can cascade heat to a lower-temperature interval or reject it to the refrigeration system. This heat surplus entry represents the maximum amount of heat that can be rejected to the refrigeration system from that temperature interval. This value is used for computing the maximum energy D_l^{\max} that can reach level l in the refrigeration system. Temperature intervals with a heat deficit can either receive heat from a higher temperature interval or the refrigeration system. These energy flows are shown as arcs in Figure 14. Energy flows between temperature intervals and energy flows between temperature intervals and the refrigeration superstructure are grouped into the arc set \mathcal{G}_e . Constraint 15 is modified as follows to account for cascading heat from higher temperature intervals

$$\sum_{m:(m,l) \in \mathcal{G}_e} D_{ml} + Q_{\text{load}} = \sum_{m:(l,m) \in \mathcal{G}_e} D_{lm} \quad \forall l \in \mathcal{L}^{\text{load}}$$

where Q_{load} is the surplus (or negative deficit) entry shown in the temperature interval TI_l in Figure 14. Summarizing, cooling loads and sinks represent the heat surplus or deficit for each temperature interval in the cascade diagram, respectively. A portion of these cooling and heating loads are satisfied by the refrigeration system, and the remaining are met by cooling water and hot utilities through cascading. This implies that the cooling/heating loads serviced by the refrigeration system are variables for which only upper bounds are known.

The presence of multiple heat sinks imply that Condition 1 is not met and, thus, Property 1 may be violated at the optimal solution. Violation of Property 1 may result in stream splitting and some nonconvex constraints from set 12, which

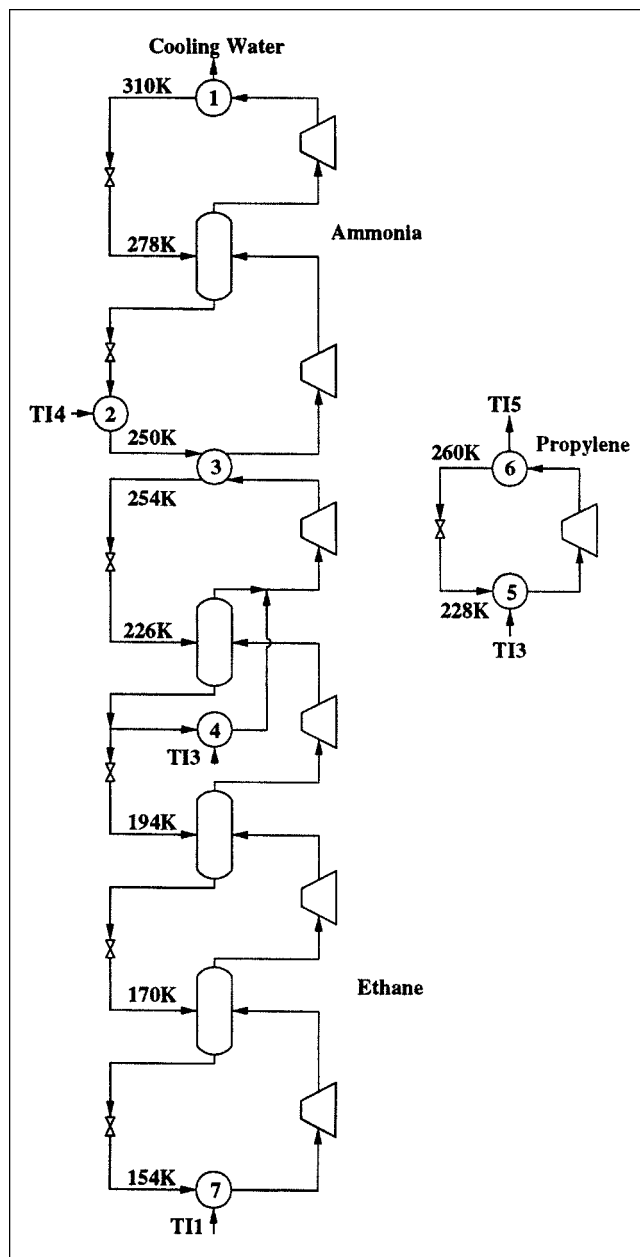


Figure 15. Minimum cost refrigeration system (4 K discretization) for Example 3.

are not redundant. First, the P_z formulation is solved with a 4 K discretization. The resulting optimal solution involves stream splitting requiring the use of the split reconciliation procedure (SRP) (see Appendix C) to properly reflect this stream splitting in the objective function. This procedure terminates in only six iterations yielding an optimal refrigeration system, which is shown in Figure 15. The interaction of the refrigeration system with the temperature interval diagram is depicted in Figure 16. The best solution for the 4 K discretization involves a cost of \$753,788/yr. The relative gap between the upper bound and the best lower bound for the 4 K discretization is 1.3%. Note that no economizers are present at the optimal solution.

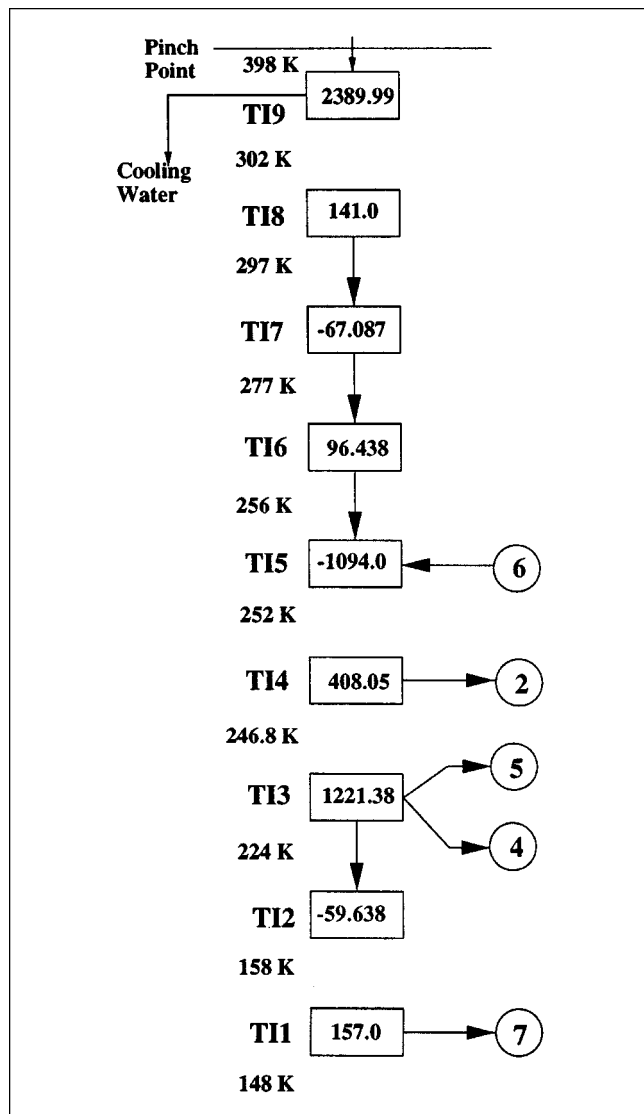


Figure 16. Interaction between temperature interval diagram and the refrigeration superstructure for Example 3.

The 1 K discretization case is solved by using the LSP($\delta n = 3$) procedure. Parameter δn is set to 3 because in going from the active levels of the optimal solution for the 4 K case to a 1 K discretization there are three unaccounted levels on each side of each active level. The LSP converged in three repetitions to a refrigeration configuration featuring stream splitting. Next, the SRP procedure is applied to the superstructure employed in the last iteration of LSP. The SRP procedure terminates in six iterations yielding an optimal solution which is shown in Figure 17. This refrigeration structure involves a cost of \$723,548/yr which is 4% less than the best solution for the 4 K discretization. The interaction of the refrigeration system with the temperature interval diagram is depicted in Figure 16. The striking feature of the configuration in Figure 17 is the disconnectedness of the propylene refrigeration cycle from the rest of the refrigeration system. This results because part of the energy from temperature interval 3 is used to satisfy the demand of temperature interval

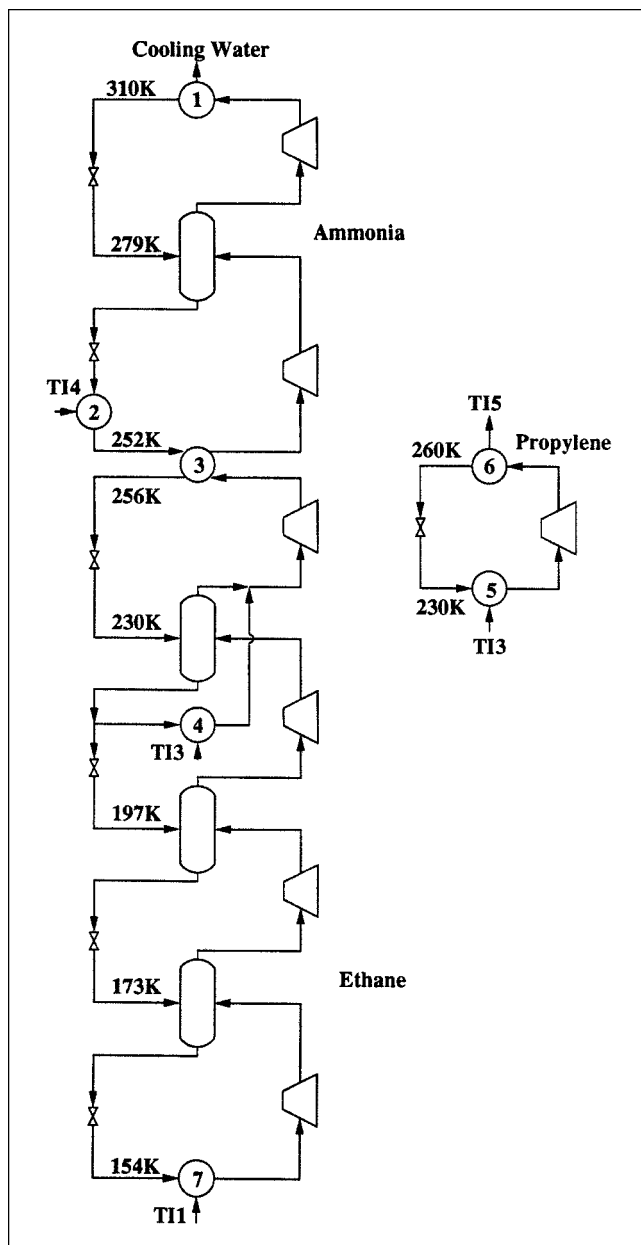


Figure 17. Minimum cost configuration obtained by local search procedure for Example 3.

5 and the rest is rejected to cooling water. Also, in this example, only three refrigerants are chosen from the available eight refrigerants. Comparison of Figure 17 with the prepostulated refrigeration structure of Colmenares and Seider (1989) reveals that the proposed methodology suggests significant structural changes, as well as different refrigerants.

Summary and Conclusions

A systematic methodology for finding the optimal refrigeration cycle topology incorporating refrigerant selection was proposed. A superstructure representation accounting for most features of complex multistage refrigeration systems was introduced. It was shown that key questions arising in the

synthesis of a refrigeration system referring to which refrigerants participate in the system, the number and temperatures of intermediate stages, the temperatures at which refrigerant switches occur, and the presence of a presaturator or an economizer at intermediate stages can be directly answered by encompassing the proposed superstructure description within an optimization framework.

The optimization formulation obtained was a nonconvex MINLP. Based on a variable projection technique, all nonlinear terms were isolated within a single constraint set. It was shown that if, after omitting the nonconvex constraint set, the energy flows form a graph with inverted arborescence (Property 1) or there are no economizers (Property 2) at the optimal solution, then the nonconvex constraint set is redundant and, thus, can be omitted yielding a MILP representation. Properties 1 and 2 were proven to hold for the case of only presaturators and single heat sinks (Condition 1). Computational tractability of the resulting MILP formulation was further enhanced by: (i) condensing the binary variables from denoting level-to-level interactions to single level activators; (ii) predetermining whether a given simple cycle features a presaturator or economizer; (iii) systematically deriving bounds on the energy flows by solving a sequence of longest and shortest path problems on the network representing the refrigeration superstructure. For the cases when Property 1 does not hold, a split reconciliation procedure (SRP) was derived which was proven to converge to the optimal solution in a finite number of steps.

Three example problems of increasing difficulty were addressed. Results from all examples unanimously suggest that complex, nonintuitive topologies and refrigeration switching patterns emerge as optimal refrigeration configurations. The second example indicated that, for very high discretizations (1 K), a local search procedure is needed. The same applied to the third example which integrated the refrigeration system with a process heat recovery network. Currently, we are exploring decomposition approaches for solving problems with very fine discretizations and modeling extensions to account for refrigerant mixtures and group contribution-based property prediction.

Acknowledgments

Financial support by the NSF Career Award CTS-9701771 and computing hardware support by the IBM Shared University Research Program 1996, 1997, and 1998 is gratefully acknowledged.

Notation

- $\alpha = \{(l, m)\}$ = arc-set of graph $\mathcal{G}(\mathcal{L}, \alpha)$ representing network superstructure
 $\alpha_e \subset \alpha = \{(l, m)\}$ = set of energy flows representing energy exchange between a process stream and a refrigerant or a switch between refrigerants
 $\alpha_c \subset \alpha = \{(l, m)\}$ = set of energy flows forming a simple cycle
 $\mathcal{L} = \{\beta\}$ = set of prepostulated temperature levels
 $\mathcal{L}^{cw} \subset \mathcal{L} = \{\beta\}$ = set of refrigerant temperature levels, rejecting energy to cooling water
 $\mathcal{L}^{int} \subset \mathcal{L} = \{\beta\}$ = set of refrigerant temperature levels, not rejecting energy to cooling water
 $\mathcal{L}^{load} \subset \mathcal{L} = \{\beta\}$ = set of temperature levels corresponding to process streams to be cooled
 $\mathcal{L}^{sink} \subset \mathcal{L} = \{\beta\}$ = set of temperature levels corresponding to process streams to be heated

$\mathcal{L}' \subset \mathcal{L} = \{\beta\}$ = set of temperature levels accepting and rejecting energy to refrigerant/process streams

Parameters

- c_{pl}^{liq} = liquid heat capacity of refrigerant ref_j
 c_{pl}^{vap} = vapor heat capacity of refrigerant ref_j
 C_c = operating cost of a compressor
 D_{lm}^U = maximum energy flow between levels l and m
 h_l^{liq} = enthalpy of saturated liquid at level l
 h_l^{vap} = enthalpy of saturated vapor at level l
 ΔH_l^{vap} = heat of vaporization of refrigerant operating at level l
 P_l = vapor pressure of refrigerant operating at level l
 ref_j = refrigerant operating at level l
 T_l = temperature of level l
 WC_{lm} = proportionality constant relating mechanical work to temperature and flow rate
 Q_l^{load} = amount of heat to be removed from a process stream (cooling load)
 Q_l^{sink} = amount of heat required by a process stream (heat sink)
 η = thermodynamic efficiency of mechanical compression
 γ_j = specific heat ratio of refrigerant ref_j

Variables

- $h_l^{c,p}$ = enthalpy of superheated stream entering level l from compressors (Figure 2, Table 1)
 h_{lm}^{out} = enthalpy of inlet stream to a compressor present in a cycle between levels l and m (Figure 2, Table 1)
 $T_l^{c,p}$ = temperature of superheated stream entering level l from compressors (Figure 2, Table 1)
 T_{lm}^{out} = temperature of inlet stream to a compressor present in a cycle between levels l and m (Figure 2, Table 1)
 y_{lm} = 0-1 variable denoting the presence or absence of a simple cycle operating between levels l and m
 z_l = 0-1 variable denoting the presence or absence of a temperature level
 μ_{lm} = refrigerant flow rate in a simple cycle operating between levels l and m
 μ'_{lm} = portion of stream μ'_l sent to level m through the block F (Figures 2, 3)
 μ''_{lm} = portion of bypass stream μ_l^b sent to level m through block F (Figures 2, 3)
 μ_l^b = flow rate of superheated vapor bypassing the vapor-liquid separator (Figure 2, Table 1)
 μ_l^v = flow rate of superheated vapor into the vapor-liquid separator (Figure 2, Table 1)
 μ_l^l = flow rate of saturated vapor leaving the vapor-liquid separator (Figure 2, Table 1)

Literature Cited

- Barnes, F. J., and C. J. King, "Synthesis of Cascade Refrigeration and Liquefaction Systems," *I&EC Process Des. Develop.*, **13**, 421 (1974).
Bazaraa, M. S., J. J. Jarvis, and H. D. Sherali, *Linear Programming and Network Flows*, Wiley, New York (1990).
Bazaraa, M. S., H. D. Sherali, and C. M. Shetty, *Nonlinear Programming: Theory and Algorithms*, Wiley, New York (1993).
Biegler, L. T., I. E. Grossmann, and A. W. Westerberg, *Systematic Methods of Chemical Process Design*, Prentice Hall, Englewood Cliffs, NJ (1997).
Brooke, A., D. Kendrick, and A. Meeraus, *GAMS: A User's Guide*, Scientific Press, Palo Alto, CA (1988).
Cheng, W. B., and R. S. H. Mah, "Interactive Synthesis of Cascade Refrigeration Systems," *I&EC Process Des. Dev.*, **19**, 410 (1980).
Churi, N., and L. E. K. Achenie, "The Optimal Design of Refrigerant Mixtures for a Two-Evaporator Refrigeration System," *Comput. Chem. Eng.*, **21**, S349 (1997).

- Colmenares, T. R., and W. D. Seider, "Synthesis of Cascade Refrigeration Systems Integrated with Chemical Processes," *Comput. Chem. Eng.*, **13**, 247 (1989).
- Daubert, T. E., and R. P. Danner, *Physical and Thermodynamic Properties of Pure Chemicals, Data Compilation*, Hemisphere Publishing Corp., New York (1989).
- Douglas, J. M., *Conceptual Design of Chemical Processes*, McGraw-Hill, New York (1988).
- Duvedi, A. P., and L. E. K. Achenie, "Designing Environmentally Safe Refrigerants Using Mathematical Programming," *Chem. Eng. Sci.*, **51**, 3727 (1996).
- Gani, R., B. Nielsen, and A. Fredenslund, "A Group Contribution Approach to Computer-Aided Molecular Design," *AIChE J.*, **37**, 1318 (1991).
- Gaubertier, J. J., and H. Paradowski, "Method and Apparatus for Cooling a Gaseous Mixture," U.S. Patent No. 4,251,247 (1981).
- Hochbaum, D. S., and A. Segev, "Analysis of Flow Problems with Fixed Charges," *Networks*, **19**, 291 (1989).
- Joback, K. G., and G. Stephanopoulos, "Designing Molecules Possessing Desired Physical Property Values," *FOCAPD '89*, Snowmass, CO, p. 363 (1989).
- Kinard, G. E., and L. S. Gaumer, "Mixed Refrigerant Cascade Cycles," *Chem. Eng. Prog.*, **69**, 56 (1973).
- Liu, Y., and J. W. Pevier, "Dual Mixed Refrigerant Natural Gas Liquefaction," U.S. Patent No. 4,545,795 (1985).
- Minieka, E., *Optimization Algorithms for Networks and Graphs*, Marcel Dekker, New York (1978).
- Paradowski, H., and J. Dufresne, "Process Analysis Shows How to Save Energy," *Hydro. Process.*, 103 (1983).
- Paradowski, H., and D. Leroux, "Method and Apparatus for Cooling and Liquefying at Least One Gas with a Low Boiling Point, Such as for Example Natural Gas," U.S. Patent No. 4,539,028 (1985).
- Shelton, M. R., and I. E. Grossmann, "A Shortcut Procedure for Refrigeration Systems," *Computers and Chem. Eng.*, **9**, 615 (1985).
- Shelton, M. R., and I. E. Grossmann, "Optimal Synthesis of Integrated Refrigeration Systems—I," *Computers and Chem. Eng.*, **10**, 445 (1986).
- Stoecker, W. F., and J. W. Jones, *Refrigeration and Air Conditioning*, McGraw-Hill, New York (1982).
- Swaney, R. E., "Thermal Integration of Processes with Heat Engines and Heat Pumps," *AIChE J.*, **35**, 1003 (1989).
- Townsend, W. D., and B. Linnhoff, "Heat and Power Networks in Process Design I: Criteria for Placement of Heat Engines and Heat Pumps in Process Networks," *AIChE J.*, **29**, 748 (1983).
- Turton, R., R. C. Bailie, W. B. Whiting, and J. A. Shaeiwitz, *Analysis, Synthesis and Design of Chemical Processes*, Prentice Hall, Englewood Cliffs, NJ (1998).
- Venkatasubramanian, V., K. Chan, A. Sundaram, and J. M. Caruthers, "Designing Molecules with Genetic Algorithms," *AIChE Symp. Ser.*, **304**, 270 (1995).
- Zubair, S. M., "Thermodynamics of Vapor-Compression Refrigeration Cycle with Mechanical Subcooling," *Energy*, **19**, 707 (1994).

Appendix A: Derivation of a Reduced Variable Basis Set

This Appendix discusses the projection of the feasible region represented by constraints 1 through 9 (see Model Formulation section) onto the reduced space of variables D_{lm} , μ_{lm} and W_{ml} . These variables will, henceforth, be referred to as the *basic* variables of the formulation and the remaining as *nonbasic*. The projection of the original feasible region

onto the space of the basic variables is accomplished by expressing the nonbasic variables in terms of basic variables and substituting these expressions in the constraint set. This implies that the values of nonbasic variables become specified once the values of basic variables are known. The main constraints in which the expression for a nonbasic variable in terms of basic variables is substituted are the nonnegativity constraints for the eliminated nonbasic variables.

The specific enthalpies h_l^{cp} and h_{lm}^{out} are expressed in terms of the basic variables using Eqs. 8 and 7, respectively and are given by

$$h_l^{cp} = \frac{\sum_{m:(m,l) \in \mathcal{G}_i} (D_{ml} + W_{ml})}{\sum_{m:(m,l) \in \mathcal{G}_i} \mu_{ml}} + h_l^{\text{liq}} \quad (\text{A1})$$

$$h_{lm}^{\text{out}} = \frac{D_{lm}}{\mu_{lm}} + h_{lm}^{\text{in}} \quad (\text{A2})$$

Analytical expressions in terms of the basic variables for the flow rates μ'_{lm} and μ''_{lm} are obtained by solving Eqs. 5 and 6

$$\mu'_{lm} = \mu_{lm} \left(\frac{h_l^{cp} - h_{lm}^{\text{out}}}{h_l^{cp} - h_l^{\text{vap}}} \right) \geq 0, \quad \forall (l, m) \in \mathcal{G}_i \quad (\text{A3})$$

$$\mu''_{lm} = \mu_{lm} \left(\frac{h_{lm}^{\text{out}} - h_l^{\text{vap}}}{h_l^{cp} - h_l^{\text{vap}}} \right) \geq 0, \quad \forall (l, m) \in \mathcal{G}_i \quad (\text{A4})$$

Note that $h_l^{cp} > h_l^{\text{vap}}$ because stream 3, formed by the mixing of the streams exiting the compressors, is superheated. Thus, nonnegativity of μ'_{lm} is ensured by imposing $h_l^{cp} \geq h_{lm}^{\text{out}}$. This can be recast using Eqs. A1 and A2 in terms of energy flows (basic variables) as

$$\frac{\sum_{m:(m,l) \in \mathcal{G}_i} (D_{ml} + W_{ml})}{\sum_{m:(m,l) \in \mathcal{G}_i} \mu_{ml}} \geq \frac{D_{lm}}{\mu_{lm}} + (h_{lm}^{\text{in}} - h_l^{\text{liq}}), \quad \forall (l, m) \in \mathcal{G}_i \quad (\text{A5})$$

Similarly, nonnegativity of μ''_{lm} is ensured by imposing the restriction $h_{lm}^{\text{out}} \geq h_l^{\text{vap}}$. In terms of energy flows (basic variables) this can equivalently be rewritten as

$$D_{lm} \geq \mu_{lm} (h_l^{\text{vap}} - h_{lm}^{\text{in}}), \quad \forall (l, m) \in \mathcal{G}_i \quad (\text{A6})$$

Analytical expressions for μ_l^j and μ_l^i are obtained by solving Eqs. 1 and 2

$$\mu_l^j = \frac{\sum_{m:(l,m) \in \mathcal{G}_i} \mu_{lm} (h_l^{\text{vap}} - h_{lm}^{\text{in}}) - \sum_{m:(m,l) \in \mathcal{G}_i} \mu_{ml} (h_l^{\text{vap}} - h_l^{\text{liq}}) + \sum_{m:(l,m) \in \mathcal{G}_e} D_{lm} - \sum_{m:(m,l) \in \mathcal{G}_e} D_{ml}}{h_l^{cp} - h_l^{\text{vap}}}, \quad \forall l \in \mathcal{L}^{\text{int}} \quad (\text{A7})$$

$$\mu_l^i = \frac{\sum_{m:(l,m) \in \mathcal{G}_i} \mu_{lm} (h_l^{cp} - h_{lm}^{\text{in}}) - \sum_{m:(m,l) \in \mathcal{G}_i} \mu_{ml} (h_l^{cp} - h_l^{\text{liq}}) + \sum_{m:(m,l) \in \mathcal{G}_e} D_{lm} - \sum_{m:(l,m) \in \mathcal{G}_e} D_{ml}}{h_l^{cp} - h_l^{\text{vap}}}, \quad \forall l \in \mathcal{L}^{\text{int}} \quad (\text{A8})$$

Therefore, nonnegativity of μ_l^i is maintained by imposing the following constraint

$$\begin{aligned} & \sum_{m:(l,m) \in \mathcal{G}_i} \mu_{lm} (h_l^{\text{vap}} - h_{lm}^{\text{in}}) + \sum_{m:(l,m) \in \mathcal{G}_e} D_{lm} \\ & \geq \sum_{m:(m,l) \in \mathcal{G}_i} \mu_{ml} (h_l^{\text{vap}} - h_l^{\text{liq}}) + \sum_{m:(m,l) \in \mathcal{G}_e} D_{ml}, \quad \forall l \in \mathcal{L}^{\text{int}} \end{aligned} \quad (\text{A9})$$

Note that mass flow rates μ_l^i and μ_l^b are always nonnegative as the sum of nonnegative variables μ_{lm}^i and μ_{lm}^b respectively (see Eqs. 4 and 3).

Thus, the nonbasic variables along with their defining equations (Eqs. 1, 2, 3, 5–8) are eliminated, while the nonnegativity restrictions (Eqs. A5, A6, A9) on the nonbasic variables are retained. Equations 4 and 9 remain, because they are not used in solving for the nonbasic variables and, thus, need to be recast in terms of the basic variables. Eliminating μ_l^i and μ_{lm}^i from Eq. 4 using Eqs. A8 and A3 gives

$$\begin{aligned} & \sum_{m:(l,m) \in \mathcal{G}_i} \mu_{lm} (h_{lm}^{\text{out}} - h_{lm}^{\text{in}}) + \sum_{m:(l,m) \in \mathcal{G}_e} D_{lm} \\ & = \sum_{m:(m,l) \in \mathcal{G}_i} \mu_{ml} (h_l^{\text{cp}} - h_l^{\text{liq}}) + \sum_{m:(m,l) \in \mathcal{G}_e} D_{ml}, \quad \forall l \in \mathcal{L}^{\text{int}} \end{aligned} \quad (\text{A10})$$

Substituting the expressions for h_l^{cp} and h_{lm}^{out} in this relation gives the more familiar relation corresponding to the overall energy balance around level l

$$\begin{aligned} & \sum_{m:(l,m) \in \mathcal{G}_i} D_{lm} + \sum_{m:(l,m) \in \mathcal{G}_e} D_{lm} \\ & = \sum_{m:(m,l) \in \mathcal{G}_i} (D_{ml} + W_{ml}) + \sum_{m:(m,l) \in \mathcal{G}_e} D_{ml}, \quad \forall l \in \mathcal{L}^{\text{int}} \end{aligned} \quad (\text{A11})$$

Equation 9 can be transformed by eliminating T_{lm}^{out} . A relation for $\mu_{lm} T_{lm}^{\text{out}}$ can be directly extracted from the expression for h_{lm}^{out}

$$\begin{aligned} D_{lm} & = \mu_{lm} (h_{lm}^{\text{out}} - h_{lm}^{\text{in}}) \\ & = \mu_{lm} (h_{lm}^{\text{out}} - h_l^{\text{vap}}) + \mu_{lm} (h_l^{\text{vap}} - h_{lm}^{\text{in}}) \\ & = \mu_{lm} c_{p_l}^{\text{vap}} (T_{lm}^{\text{out}} - T_l) + \mu_{lm} (h_l^{\text{vap}} - h_{lm}^{\text{in}}), \quad \forall (l, m) \in \mathcal{G}_i \end{aligned}$$

Therefore, the expression for $\mu_{lm} T_{lm}^{\text{out}}$ is

$$\begin{aligned} \mu_{lm} T_{lm}^{\text{out}} & = \left(\frac{1}{c_{p_l}^{\text{vap}}} \right) \left[D_{lm} - \mu_{lm} (h_l^{\text{vap}} - h_{lm}^{\text{in}} - c_{p_l}^{\text{vap}} T_l) \right], \\ & \quad \forall (l, m) \in \mathcal{G}_i \end{aligned}$$

Hence, the compression work $W_{lm} = WC_{lm} \mu_{lm} T_{lm}^{\text{out}}$ is given by the following linear relation

$$W_{lm} = \left(\frac{WC_{lm}}{c_{p_l}^{\text{vap}}} \right) \left[D_{lm} - \mu_{lm} (h_l^{\text{vap}} - h_{lm}^{\text{in}} - c_{p_l}^{\text{vap}} T_l) \right], \quad \forall (l, m) \in \mathcal{G}_i$$

The expression $(h_l^{\text{vap}} - h_{lm}^{\text{in}})$ in terms of latent heat of vaporization and liquid heat capacity is given by $[\Delta H_l^{\text{vap}} - c_{p_l}^{\text{liq}}(T_m - T_l)]$ (Shelton and Grossmann, 1985).

Additional constraints include

$$Q_l^{\text{load}} = \sum_{m:(m,l) \in \mathcal{G}_e} D_{lm}, \quad \forall l \in \mathcal{L}^{\text{load}}$$

which ensures that the refrigeration system meets the cooling loads and

$$Q_l^{\text{sink}} = \sum_{m:(l,m) \in \mathcal{G}_e} D_{ml}, \quad \forall l \in \mathcal{L}^{\text{sink}}$$

which guarantees that the heat requirements of process streams acting as heat sinks is satisfied by the refrigeration system. Finally, logical constraints

$$D_{lm} \leq D_{lm}^U y_{lm}, \quad \forall (l, m) \in \mathcal{G}_i$$

force the energy flow within a simple cycle to zero if the cycle does not exist. To safeguard against the unrealistic configuration involving two consecutive refrigerant switches without having at least one simple refrigeration cycle operating between them the following constraints are added

$$\begin{aligned} \sum_{m:(m,l) \in \mathcal{G}_e} D_{ml} & \leq \sum_{m:(l,m) \in \mathcal{G}_i} D_{lm}, \quad \forall l \in \mathcal{L}' \\ \sum_{m:(l,m) \in \mathcal{G}_e} D_{lm} & \leq \sum_{m:(m,l) \in \mathcal{G}_i} (D_{ml} + W_{ml}), \quad \forall l \in \mathcal{L}' \end{aligned}$$

Note that these constraints are required only for the set of levels \mathcal{L}' which can both receive and reject energy to process streams/refrigerants.

Appendix B: Proof of Condition 1 Implying Property 1 for Concave Investment Costs

As discussed in Appendix B, it suffices to characterize the optimal solutions for D_{lm} for any given feasible temperature level activation (fixed z_l). Condition 1 implies the presence of only presaturators and no economizers. Therefore, the constraint set simplifies as follows after the binary variables z_l are fixed at a feasible assignment and economizers are excluded

$$\begin{aligned} \sum_{m:(l,m) \in \mathcal{G}_e} D_{lm} & = Q_l^{\text{load}}, \quad \forall l \in \mathcal{L}^{\text{load}} \\ \sum_{m:(l,m) \in \mathcal{G}_i} D_{lm} + \sum_{m:(l,m) \in \mathcal{G}_e} D_{lm} - \sum_{m:(m,l) \in \mathcal{G}_e} D_{ml} \\ & - \sum_{m:(m,l) \in \mathcal{G}_i} (1 + \alpha_{ml}) D_{ml} = 0, \quad \forall l \in \mathfrak{N}^{\text{presat}} \\ D_{ml} & \geq 0, \quad \forall (l, m) \in \mathcal{G}_i' \end{aligned}$$

where $\mathcal{L}^{\text{load}}$ is the set of nodes corresponding to loads, and $\mathcal{N}^{\text{presat}}$ is the set of intermediate nodes (presaturators) excluding the single condenser. These three constraint sets include energy balances for levels incurring cooling loads, energy balances for intermediate levels, and the nonnegativity restriction on the energy flows. This yields a polytope, because all energy flows have finite lower and upper bounds. Therefore, the optimization problem at hand minimizes a concave objective function over a polytope. This means that there exists an extreme point optimal solution (Bazaraa et al., 1993). Hence, the validity of Property 1 given Condition 1 can be established by characterizing the extreme points (basic feasible solutions) of the feasible region.

The constraint set defining the feasible region possesses a generalized network problem structure, because each variable appears in at most two constraints other than the nonnegativity constraints (Bazaraa et al., 1990). Assuming that the constraint set is of full rank, each component of the subgraph corresponding to the basic feasible solution is either a rooted tree or has exactly one cycle (Bazaraa et al., 1990). A rooted tree implies a tree with one root arc. Full-rankness of the constraint set is straightforward to show [see Bazaraa et al. (1990) for derivation for the pure network case] by finding a lower triangular submatrix with nonzero diagonal elements. In the context of the above defined constraint set, a root arc is one that links an intermediate level with the *single* condenser. The *inverted arborescence* property at the optimal solution can then be shown by contradiction. Consider a solution in which energy flow from a given level splits. Since the energy eventually reaches the condenser, one of the following cases must occur:

(1) The split energy flows reach the condenser using different paths. Since each arc reaching the condenser is a root arc, this implies that there is a connected subgraph with more than one root arc. This does not correspond to a basic feasible solution.

(2) The split energy flows combine before reaching the condenser. This implies that the connected subgraph contains a cycle and a root arc. This again does not correspond to a basic feasible solution.

Hence, a solution in which energy flow from a given level splits is not an extreme point. Equivalently, since there exists an extreme point optimal solution to the problem, there exists an optimal solution for which property 1 holds. Therefore, Condition 1 implies Property 1 (inverted arborescence) even for concave investment costs.

Appendix C: Splitting Reconciliation Procedure

This appendix discusses how stream splitting at the optimal solution of P_z is dealt when Property 1 is not satisfied. In this case an iterative procedure is proposed which solves formulation P_z augmented with the binary variables y_{lm} for the levels which exhibited stream splitting in the previous iterations. Computational experience indicates that only up to a handful of levels may involve stream splitting requiring only a few additional y_{lm} variables per iteration. The procedure is shown to converge in a finite number of iterations to an optimal solution which does not involve stream splitting at levels that are not described by the level-to-level binary variables y_{lm} . In

fact, it is shown that this optimal solution is rigorously equal to the optimal solution of P .

The optimization problem at iteration k involves the following new objective function and logical constraints. The remaining constraints are unaffected and thus are not listed.

Formulation (P_z^k)

$$\min \sum_{l \in \mathcal{L}^{\text{int}}} C_f z_l + \sum_{(l,m) \in \mathcal{A}_i^k} C_f y_{lm} + \sum_{(l,m) \in \mathcal{A}_i} (C_v + C_e) W_{lm}$$

subject to

$$D_{lm} \leq D_l^{\text{max}} y_{lm} \quad \forall (l,m) \in \mathcal{A}_i^k$$

$$\sum_{m:(l,m) \in \mathcal{A}_i \setminus \mathcal{A}_i^k} D_{lm} \leq D_l^{\text{max}} z_l \quad \forall l \in \mathcal{L}^{\text{int}}$$

where \mathcal{A}_i^k is the set of arcs corresponding to the added y_{lm} variables. Note that $\mathcal{A}_i^k = \mathcal{A}_i$ corresponds to (P) and $\mathcal{A}_i^k = \emptyset$ corresponds to P_z .

The iterative scheme proceeds as follows:

(i) $k = 1$. Set $\mathcal{A}_i^1 = \emptyset$.

(ii) Solve (P_z^k). Let the optimal value be $v(P_z^k)$ and $\bar{\mathcal{A}}$ be the arcs for which $W_{lm} > 0$. If $v(P_z^k) = \sum_{(l,m) \in \bar{\mathcal{A}}} [C_f + (C_v + C_e)W_{lm}]$, then stop. Otherwise go to Step (iii).

(iii) Consider levels l where the energy flow splits, and it is directed to more than one refrigerant level. Let the arcs corresponding to the energy flows between such levels be \mathcal{A}' . Augment $\mathcal{A}_i^{k+1} = \mathcal{A}_i^k \cup \mathcal{A}'$. Set $k = k + 1$ and go to step (ii). This procedure terminates finitely, because at each iteration either a y_{lm} is added to the formulation or the procedure terminates.

Next, it is shown that at every iteration k $v(P_z^k)$ is a valid lower bound to $v(P)$, which is the optimal solution of (P). It suffices to show that a solution to (P_z^k) which is at least as good as the optimal solution to (P) can be constructed. Suppose that the optimal solution to (P) is $(\bar{D}_{lm}, \bar{W}_{lm}, \bar{\mu}_{lm}, \bar{y}_{lm})$. Let $\bar{\mathcal{A}}$ be the set of arcs for which $\bar{y}_{lm} = 1$. Then, the solution $(\bar{D}_{lm}, \bar{W}_{lm}, \bar{\mu}_{lm}, \bar{z}_l, \bar{y}_{lm})$ is feasible to (P_z^k) where

$$z_l = \max_{m:(l,m) \in \bar{\mathcal{A}} \setminus \mathcal{A}_i^k} \bar{y}_{lm}$$

The objective value $v(P_z^k)$ is given by

$$v(P_z^k) = \sum_{l \in \mathcal{L}^{\text{int}}} C_f \bar{z}_l + \sum_{(l,m) \in \mathcal{A}_i^k} C_f \bar{y}_{lm} + \sum_{(l,m) \in \bar{\mathcal{A}}} (C_v + C_e) \bar{W}_{lm}$$

Because

$$\max_{m:(l,m) \in \bar{\mathcal{A}} \setminus \mathcal{A}_i^k} \bar{y}_{lm} \leq \sum_{m:(l,m) \in \bar{\mathcal{A}} \setminus \mathcal{A}_i^k} \bar{y}_{lm}$$

we have

$$\begin{aligned}
\nu(P_z^k) &\leq \sum_{(l,m) \in \bar{\alpha} \setminus \alpha_i^k} C_f \bar{y}_{lm} + \sum_{(l,m) \in \alpha_i^k} C_f \bar{y}_{lm} \\
&\quad + \sum_{(l,m) \in \alpha_i} (C_v + C_e) \bar{w}_{lm} \\
&= \sum_{(l,m) \in \bar{\alpha}} C_f \bar{y}_{lm} + \sum_{(l,m) \in \alpha_i} (C_v + C_e) \bar{w}_{lm} \\
&= \nu(P)
\end{aligned}$$

Therefore, because a feasible solution to (P_z^k) has a lower objective value than (P) , the optimal solution value to (P_z^k) for every iteration k is a valid lower bound for (P) . In addition, since (P_z^k) and (P) share the same set of feasible energy flows, the optimal energy flow vector from (P_z^k) can be used to obtain an upper bound for $\nu(P)$. This upper bound is equal to the optimal solution value of (P_z^k) with the addition of the fixed-term charges for the unaccounted arcs by formulation (P_z^k) . More importantly, at termination $\nu(P_z^k)$ matches the cost of a feasible solution. Therefore, $\nu(P_z^k)$ is also an upper bound for $\nu(P)$. Therefore, $\nu(P_z^k)$ must be equal to $\nu(P)$.

Appendix D: Longest and Shortest Path Problems

The LP formulation for the longest path problem is given by (Bazaraa et al., 1990)

$$\max z = \sum_{(l,m) \in \alpha_i} \ln(1 + w_{lm}^U) x_{lm}$$

subject to

$$\begin{aligned}
\sum_{m:(l,m) \in \alpha} x_{lm} - \sum_{m:(m,l) \in \alpha} x_{ml} &= \begin{cases} |\mathcal{L}| - 1, & \text{if } l = 1 \\ -1, & \text{Otherwise} \end{cases} \\
x_{lm} &\geq 0
\end{aligned}$$

Here, x_{lm} denote the arc flows in the graph with arc costs given by $\ln(1 + w_{lm}^U)$. The constraint set for the shortest path problem is the same, but the objective is to minimize, and the cost of each arc is given by $\ln(1 + w_{lm}^L)$. The shortest or the longest path can be obtained from the solution using the dual variables w_l of the constraints. Specifically, the longest path from node 1 to any node l is given by $w_l - w_1$. Since this

corresponds to $\sum_{(l,m) \in \phi} \ln(1 + w_{lm}^U)$ for the optimal path, D_l^{\max} can be computed as follows

$$D_l^{\max} = Q^{\text{load}} e^{(w_1 - w_l)}$$

The same expression gives D_l^{\min} when the dual variables from the shortest path problem are used.

If circuits are present in the graph $\mathcal{G}(\mathcal{L}, \alpha)$, then the LP formulation for the longest path problem will be unbounded. To remedy this, an ordering of refrigerants in the ascending order of normal boiling points is used. This implies that every refrigerant switch occurs between a refrigerant with a lower normal boiling point rejecting heat to a refrigerant with a higher normal boiling point. This ordering precludes the presence of any circuits in $\mathcal{G}(\mathcal{L}, \alpha)$.

Furthermore, only the set of nodes which are reachable from node 1 must be included in the formulation. Otherwise, the LP formulation will be infeasible. To identify the unreachable nodes, the following procedure (Bazaraa et al., 1990) must be followed before solving the longest path problem:

- (1) Construct a new graph from $\mathcal{G}(\mathcal{L}, \alpha)$ by adding a sink node and connecting all nodes except node 1 to the sink node.
- (2) Set an upper bound of one to the flow on the newly added arcs.
- (3) Solve a maxflow problem to determine the maximum flow from node 1 to the sink node in the new graph.
- (4) The set of unreachable nodes are those for which the arc connecting the node to the sink node has a zero flow at the optimal solution.

This also aids in preprocessing the superstructure since the set of nodes unreachable from all the nodes which correspond to cooling loads can be eliminated from the superstructure along with their incident arcs. It should be noted that it is not necessary to solve the maxflow problem if (Bazaraa et al., 1990) the label setting (Dijkstra's Algorithm) and correcting algorithms for the shortest and the longest path problems are directly implemented. Finally, D_l^{\max} calculated this way is a rigorous upper bound, but D_l^{\min} calculated is rigorous provided that energy from a level goes to only one level.

Manuscript received Oct. 6, 1998, and revision received Feb. 26, 1999.